European Commission

JRC TECHNICAL REPORTS

Mékrou Project

Water for growth and poverty reduction in the Mékrou transboundary river basin (Burkina Faso, Benin and Niger)

ATLAS of Thematic Maps
Contribution to the Baseline Report v.1

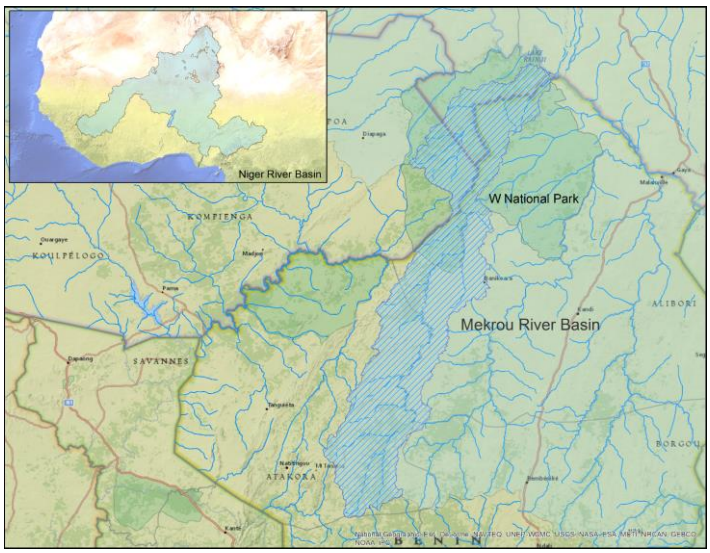

Authors: Projet Mékrou

Global Water Partnership

February 2016

Limited Distribution

Joint Research Centre

Table of Contents

1 Introduction

The Mékrou River basin, one of the six tributaries of the middle Niger basin, is shared between three countries (Benin, Burkina Faso and Niger) and is characterised by the underdevelopment of its water infrastructure. This presents significant social, economic, environmental and political risks. Furthermore the region's weak capacity to buffer the effects of hydrological variability generates uncertainty and risks for economic activities. As water becomes scarcer compared to its rising demand, there are emerging fears of potential transboundary water conflicts, which will likely constrain the region's growth. In this sense, there is a need in the region for increasing the long-term sustainability of agriculture and to foster integrated growth in all fields by developing resources, especially in the areas of energy, water resources, forestry exploitation, transport, communication and industry.

One of the fundamental aspects to start tackling all those issues is the need to understand the current status and provide an overview on different topics that affect the basin and define a baseline situation. To do so, an inventory of available datasets covering each of the sectors that have a relevant role in the region is needed, and so identify, gather and organize data available, both publicly and within the responsible national, regional and local organizations is crucial to fulfil future model requirements. This first attempt will serve to provide a frame under which the future water management system will be developed. This will be aimed at providing seamless integration of existing datasets and models, turning to be a common open platform for spatial decision making. In this sense the concept of system openness refers to the flexibility leading to the capability of integrating new knowledge in the analysis process at any later stage.

This document covers topics related to, among others, data related to the general status of the environment including climate, geology and soils, hydrology, hydrogeology, soils, land cover, etc. as well as additional added value maps that will serve as a discussion basis and will facilitate the identification of drawbacks and advantages related to future developments. Most of the collected data is presented as a compendium of maps that have been added in the document but are also available at the 'Mékrou Water4Growth Group´ within the Aquaknow platform managed by the JRC. Along with the maps, a brief description of data sources and their characteristics, as well as a description and general statistics of the study area are presented. In order to have a harmonized set of information sources, there is an ongoing activity related to the development and setup of a geodatabase for the storage of all current and future data. Together with the geodatabase setup, the development of a Geographical Information System is also being carried out. Such a system will be accessible by users using dedicated GIS services (i.e. WMS, WFS) according to Open Geospatial Consortium standards that allows data visualization, querying and optionally, editing.

Finally, it should be taken into account the coarse resolution of some datasets, thus caution must be paid when interpreting some outcomes at local scale. However, this document should be considered as a "live" document, meaning that new maps will be generated as new data is identified and processed.

2 List of Maps/Data sets

TYPE	*SUB-TYPE*	*DESCRIPTION*	*READY*	*2016*
Management	Boundaries	Area of Interest	●	
		Area of Influence	●	
		Administrative areas	●	
		Villages/Settlements	●	
		Ethnic groups		●
		Parks, reserves, Protected areas	●	
		Water Management boundaries		●
		Agro-Ecological zones		●
		Ecological Zones	●	
		Cadastral maps		●
	Infrastructures	Roads	●	●
		Accessibility	●	
		Electricity		●
		Distribution of irrigation equipment	●	●
	Water	Pipelines		●
		Water management	●	●
		Dams, water reserves and wells		●
		Measurement equipment		●
		Water use	●	●
		Water availability index	●	
	Agriculture	Crop	●	
		Crop management	●	
		Crop productivity under different irrigation scenarios	●	
		Sowing and harvesting dates Crop management scheduling dates	●	
		Fertilizer use by crop (N & P input)	●	
	Livestock	Demand and distribution		●
		Nomadic animal breeding, distribution of herds movement trajectories		●
	Others	Wood production		●
		Fire detection		●

TYPE	*SUB-TYPE*	*DESCRIPTION*	*READY*	*2016*
Biophysical	Land Cover/Use	Land Cover/Use	●	●
		Wetlands	●	
		Water bodies	●	
		Forest change	●	
		Extension of arable land	●	
		Extension of representative crops		●
		Ground-truth information		●
		Vegetation (Leaf Area Index)		●
		NDVI	●	
	Soils	Soil data	●	
		Soil characteristics	●	
	Geology	Lithology	●	
		Lineaments (faults, cracks, folds)	●	
	Hydrogeology	Ground water distribution	●	●
		Aquifers and their potential		●
		Distribution of drillings with indication of their success or failure		●
		Depth to the water table	●	●
		Specific discharge/productivity		●
	Digital Elevation Models and derived + Hydrology	DEM	●	
		Regional sub-basin distribution	●	
		Watersheds/catchments	●	
		Water courses (main streams and tributaries, river network)	●	
		Water Resources availability	●	
		Discharge	●	●
		Slope/Aspect/Hillshade	●	
		River upstream area	●	
		Erosion risk	●	
		Potential flooding risk (floodplains)	●	
	Climatic variables	Precipitation/Temperature	●	
		Other meteorological data	●	
		Global Meteo Forcing Dataset	●	
		CRU monthly dataset (8 climate variables)	●	

Limited Distribution

TYPE	*SUB-TYPE*	*DESCRIPTION*	*READY*	*2016*
		ET/PET	●	
		Map of budyko balance		●
	Climate change scenarios	Projected changes in Prec. And Temp.		●
		Projected changes in PET		●

Table 1. List of Maps of the Atlas: some maps will be made available during 2016. Maps marked in both columns are meant to be updated if more reliable data is available.

3 General Context

The Mékrou river basin is located in the Middle Niger section which is between the Inner Delta and the Lower Niger. The Middle Niger receives six tributaries that originate in Burkina-Faso: Gorouol, Dargol, Sirba, Goroubi, Diamangou and Tapoa, and three that originate in Benin: Alibori, Sota and the Mékrou. The latter flows South-North direction in a 10860 km^2 basin which has an extension of about 290 km (S-N) and approximately 50 km in its wider cross-section and 16 km in the narrower (W-E). It´s a transboundary basin shared by three countries: Benin with the 80% of the area or 8570 km^2, Niger with 1269 km^2 and Burkina Faso with 1022 km^2, so covering each approximately the 10% of the total.

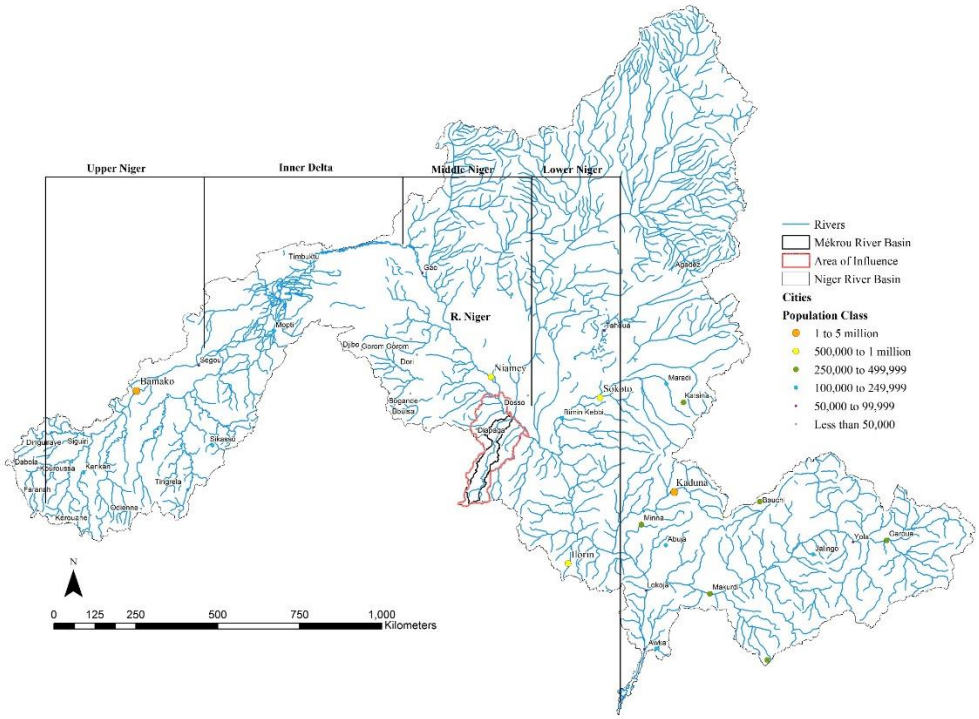

Figure 1. Niger River Basin

Since the aim of the Mékrou project is not only to stablish and describe the effects and linkages between the physical processes within the basin (Area of Interest), but as it also takes into account socioeconomic factors that aren´t strictly linked to the boundaries where those physical phenomena occur, the study area has been expanded to what it was called the Area of Influence (red line in the Administrative Boundaries Map).

According to the Global database on Administrative Areas [1], the Area of influence is comprised of 12 administrative figures (7 within the area of interest): 3 in Niger and Burkina Faso and 5 in Benin (Figure 2, Table 2). It should be taken into account that depending on the country, the GADM database is not homogeneous in its higher level administrative boundaries definition, so caution must be paid in those figures. In this sense, areas within Niger, with a total of 9942 km^2 and within Benin with 17200 km^2 are divided in "communes", while Burkina Faso´s higher levels are represented as "departments" with 5200 km^2.

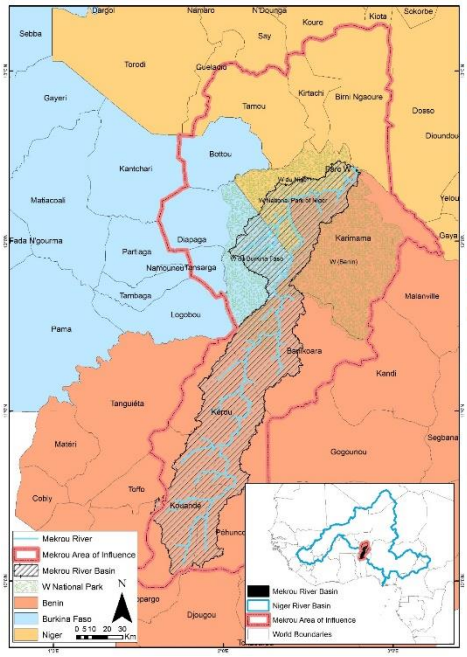

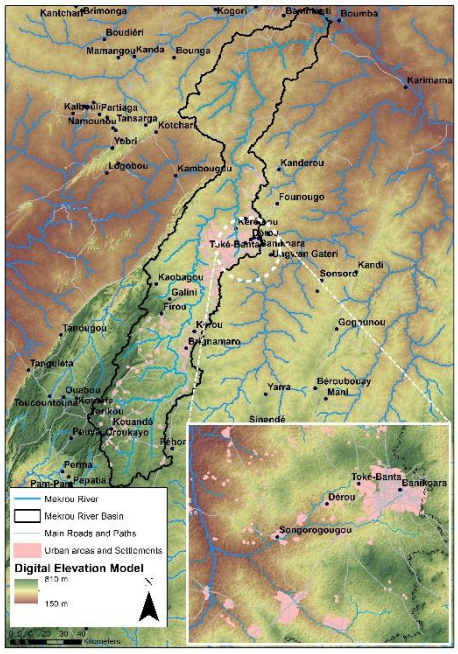

Figure 2. Administrative Boundaries Figure 3. Settlements, Roads and River Network

Country	Name	Admin Lvl 1	Admin Lvl 2	Type	Area (sq km)
Niger	Kirtachi	Tillabéry	Kollo	Commune	1026
Niger	Tamou	Tillabéry	Say	Commune	2792
Niger	Birni Ngaoure	Dosso	Boboye	Commune	3783
Niger	Parc W	Tillabéry	Say	Commune	2341
Burkina Faso	Bottou	Tapoa	Bottou	Department	1873
Burkina Faso	Diapaga	Tapoa	Diapaga	Department	3086
Burkina Faso	Tansarga	Tapoa	Tansarga	Department	219
Benin	Karimama	Alibori	Karimama	Commune	5921
Benin	Banikoara	Alibori	Banikoara	Commune	4327
Benin	Kérou	Atakora	Kérou	Commune	3042
Benin	Kouandé	Atakora	Kouandé	Commune	2050
Benin	Péhunco	Atakora	Péhunco	Commune	1872

Table 2. Administrative boundaries in the Area of Interest and Influence. Names marked with asterisks are those which are within the basin boundaries.

The Mékrou is also included in an important protected area in its northern region, the "W Transboundary Park" (IUCN Category II), which is a portion of the WAP ecological complex (W-Arly-Pendjari, Figure 4) [2]. The WAP is a mix of terrestrial, semi-aquatic, and aquatic ecosystems and is one of the largest contiguous protected areas in Africa (31000 km^2 or 50000 km^2 if riparian areas are included). Constitutes a refuge for most of the vulnerable and/or threatened animal species in the three above mentioned countries and has a dual characteristic: that is within the ecological transition zone between the Sudanese and the Sahelian area in one hand, and that is under a strong human pressure around its periphery (see Land Cover section), making the WAP complex a unique element for the conservation of savannah ecosystems [3].

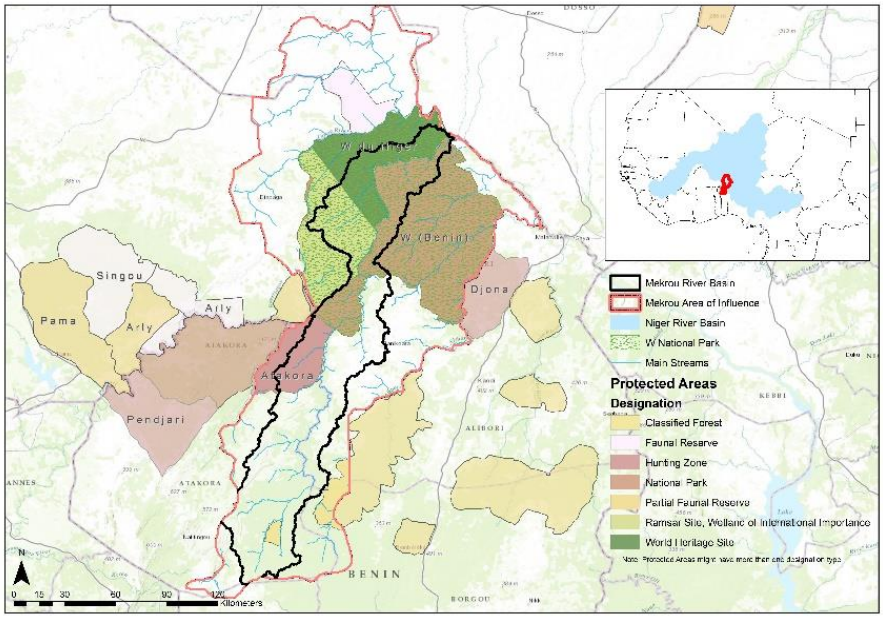

Figure 4. Boundaries (Mekrou Area of Interest, Area of Influence and Protected zones)

The importance of such protection figures will determine future decisions regarding land conservation and water management initiatives and cooperation agreements, such as the construction of the Dyodyonga Dam on the Benin-Niger border [4].

Population, inhabited areas and routes

At 30 arc-second (approximately 1km at equator) resolution, LandScan (Figure 5) is a global population distribution map that represents an "ambient population" (average over 24 hours). It is a spatially explicit raster grid computed at global scale that used an innovative approach based on Geographic Information and Remote Sensing data [5]. This map can be used to get a first idea about main population settlements and analyse if there are any linkages with land transformation and other economic activities within the basin.

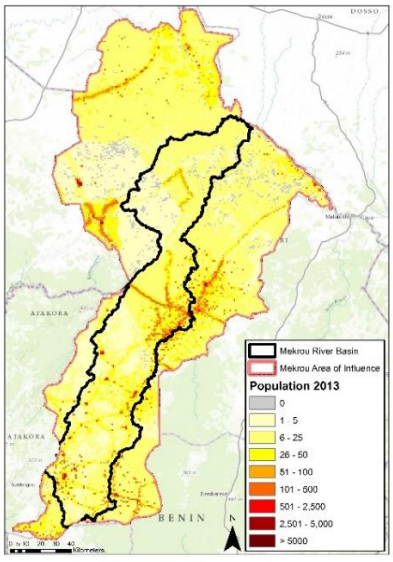

Figure 5. Population (LandScan 2013)

Limited Distribution

The most populated region is Banikoara, which is approximately located in the mid-western part of the basin and presents many villages and settlements around the main cities. In the southern region, Péhunko and Kouandé also show higher population densities compared to the northern part where the W Park is located.

As the procedure to compute this data set is based on models and uses mid-low resolution inputs, the map might not show accurately the real situation, but can serve to get a rough idea on population distribution across the basin. Considering that there is a need to better understand the location of the main cities and the general composition of other less populated settlements in the different regions that might contribute to the basin economic development, a digitization exercise was carried out in order to start building a preliminary database on this topic. Main roads including some secondary and tertiary pathways and routes were also digitized to see the connections between the previous and a detailed vector layer representing the Mékrou River was also created. This first approach to better understand these features will allow a more accurate understanding of the population distribution as well as the interactions between them and will be completed with local information when available.

In this regard, some dwellings in the area of influence are simple ground level building or just huts (Figure 6) and cannot be easily detected with coarse resolution remote sensing imagery, thus higher resolution images such as Google (2013), BING (2011), ESRI (2009) and additional sources like Open Street map have been used as base maps.

The entire territory was scanned (Figure 7) and approximately every aggregations of 3 or more houses/huts were outlined with a convex hull approach to minimize the area not covered by the buildings. When possible the areas were named with their local names using OSM as information source or other information provided by local consultants. Roads, routes and pathway were digitized and classified by width and importance based on their connection between villages. Figure 7 shows a general overview of the entire digitized area as well as some more detailed outputs that are focused on main cities within the area of influence.

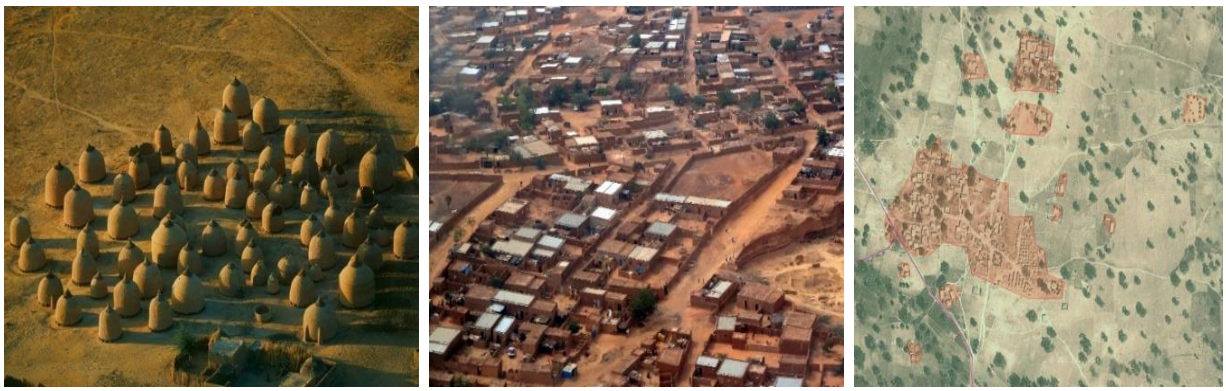

Figure 6. The house typology found in the area of influence are huts or brick and mortar buildings.

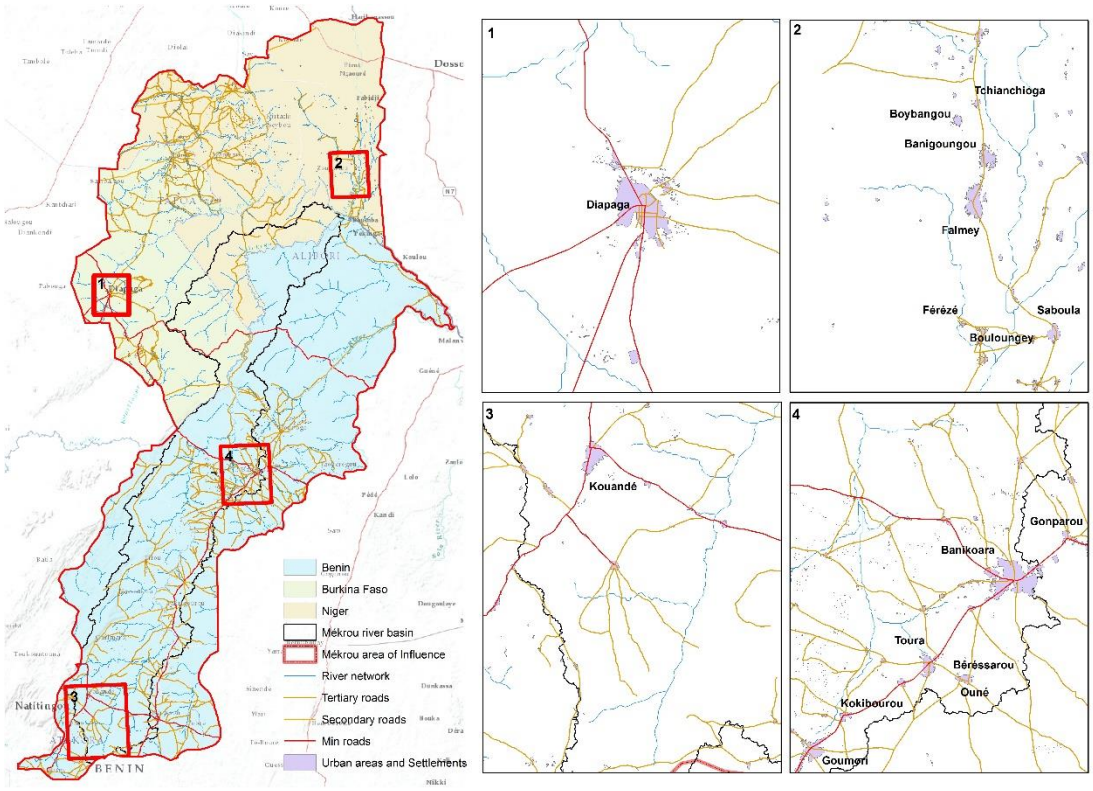

Figure 7. Digitized settlements, roads and river network

In addition, figure 8 represents an accessibility map provided by the Joint Research Centre that was made for the World Bank´s World Development report 2009 *Reshaping Economic Geography* [6]. It shows an urban/rural population gradient around lager cities of 50000 or more people, thus shows travel time to major cities. The new set of digitized information could help building more accurate accessibility maps.

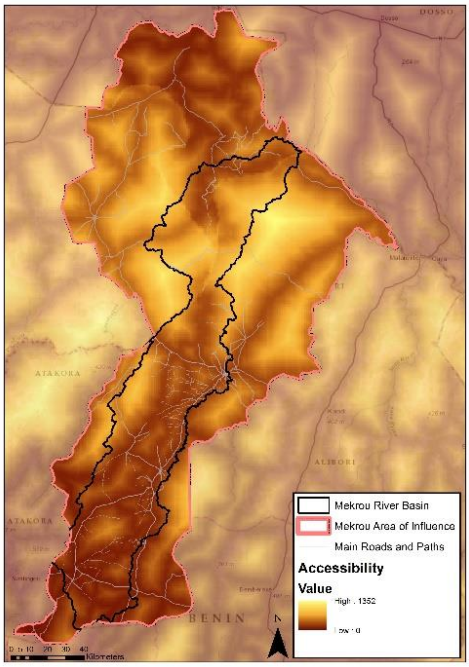

Figure 8. Accesibility map

4 Environmental features of the study area

4.1 General characteristics of the Sudano-Sahelian Ecological Zone

The seasonal patterns and amount of rainfall in the region depends on the latitude and the position of ITCZ (intertropical convergence zone), which migrates from 5 N (December to March) to 20 N (July-August). The Mékrou basin is located in the Sudano-Sahelian ecological zone and it´s within the upper infratropical belt corresponding to dry and semi-arid ombrotypic regions. The Sudanian zone extends from the north of Guinea and Côte d'Ivoire to the south of Mali in the west and again in the north of Nigeria in the East. Annual precipitation ranges from 750 to 1 500 mm, with a 5 to 7 month rainy season. The Sahelian/sub-desert zone covering the Central Delta and the river downstream from it in Mali and Niger. Precipitation ranges from 250 to 750 mm, with one rainy season of 3 to 4 months.

The main vegetation macro-group [7] within the area of interest corresponds to the **Sudano-Sahelian Treed Savanna** (Figure 9)**.** In the transition belt known as the Sudan-Sahel region, the southernmost part is the moister with 5-25% tree cover, >5 m high of Prosopis africana, Vitellaria paradoxa, Parkia biglobosa, Acacia seyal, and Faidherbia albida. This macrogroup covers the treed savanna communities that grow in the Sudano-Sahelian and Sudano-Guinean areas which have an average annual rainfall of 500-1000 mm between May-June and September-October. These savannas undergo an annual dry period of 6-8 months and are subject to strong water stresses that vary in time and space. The transitions between treed, shrub and grass savannas are also due to landscape position, soils and history of land use. The soil capacity to retain moisture determines the density of the woody cover, as well as the density and composition of the herbaceous cover. Vertisols and ferrugineous soils are moister and vary between 20 and 50% of woody cover. In these conditions, the grasses that thrive and dominate are Loudetia togoensis, Andropogon pseudapricus, Sporobolus festivus, Panicum laetum, Fimbristylis hispidula, and Spermacoce filifolia.

Other macrogroups correspond to:

North Sahel Treed Steppe & Grassland

This macrogroup corresponds to the northern, drier portion of the Sahel region, the Sahel-Sahara grass and treed steppe, with a mean annual rainfall of 100-200 mm. It groups the semi-desert natural communities of the southern portion of the South Saharan Steppe and Woodlands ecoregion (WWF) that extends in a narrow band from central Mauritania, through Mali, southwestern Algeria, Niger, Chad, and across Sudan to the Red Sea, covering the southern fringes of the Sahara Desert. Rainfall occurs mainly during the summer months of July and August, but is unreliable and varies greatly from year to year. In the north it stops at the 100-mm rainfall isohyet which is the northern limit of summer grassland pasture composed of the grasses Eragrostis, Aristida, and Stipagrostis spp. with the herbs Tribulus, Heliotropium, and Pulicharia. Woody species include Acacia tortilis, Acacia ehrenbergiana, Balanites aegyptiaca, and Maerua crassifolia, which mainly grow along wadis. In the south, the vegetation of the ecoregion grades into the Sahelian Acacia Savanna ecoregion, and includes steppes of Panicum turgidum, a perennial tussock grass.

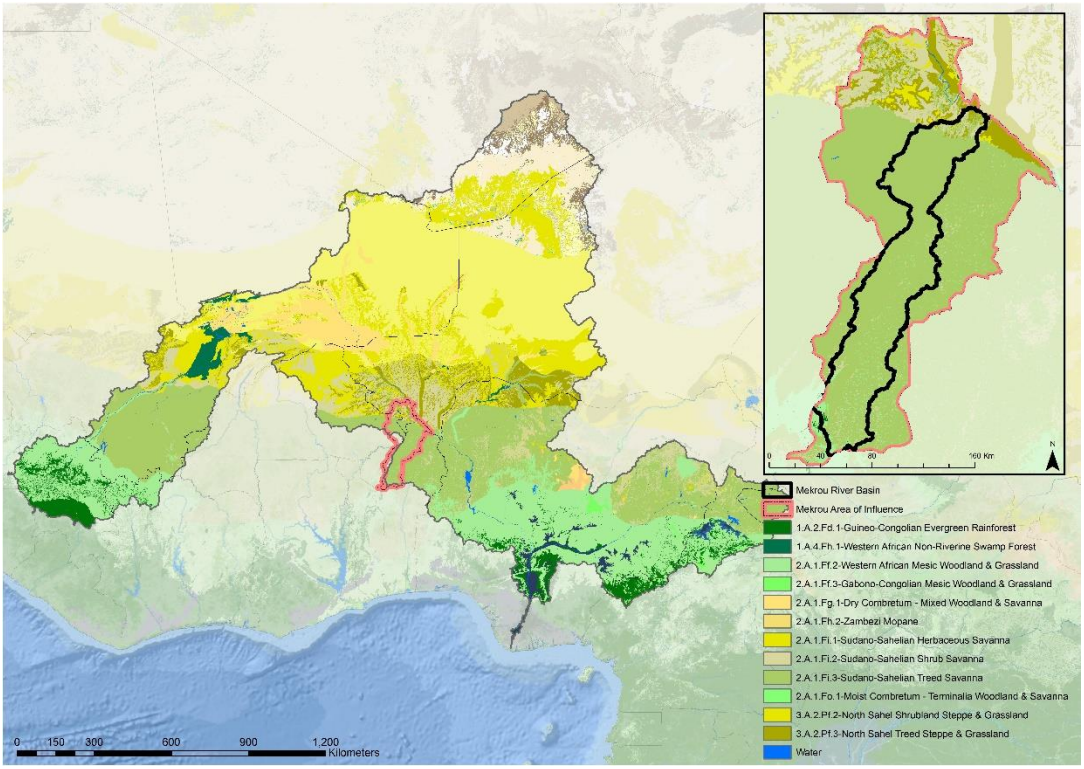

Figure 9. Vegetation Macrogroups (Labeled ecosystems-Global Ecological Land Units)

Sudano-Sahelian Shrub Savanna

This macrogroup represents the mesic portion of the transition belt with mean annual precipitation of around 500 mm and a shrub layer of 5-25% cover, less than 5 m high. Andropogon gayanus and Zornia glochidiata are representative grasses of this zone, and Combretum glutinosum, Combretum nigricans, Piliostigma reticulatum, Guiera senegalensis, and Acacia seyal are characteristic tree and shrub species.

Sudano-Sahelian Herbaceous Savanna

This macrogroup corresponds to the Sahel proper, mostly distributed in Senegal, Mauritania, Mali, Burkina Faso, Niger, and Chad. Mean annual precipitation is 200-400 mm. Although precipitation varies with latitude and local conditions, it is generally restricted to a period of 3-5 months. Storms are frequently violent in nature and the rain is often erratically distributed, both in terms of when and where it falls, with variability increasing from south to north within the Sahel. Most of the Sahel lies below 400 m in elevation. Soils vary from silty to weakly developed sandy soils on shifting and stabilized sands in the north. The vegetation is a very open savanna where grasses dominate, with a woody cover of <10%. Annuals such as Aristida adscensionis, Aristida funiculata, Panicum laetum, and Schoenefeldia gracilis are found on silty soils; Aristida mutabilis, Cenchrus biflorus, Tribulus terrestris, and Pennisetum pedicellatum are found on sandy soils. Common woody species are Acacia ehrenbergiana, Acacia laeta, Acacia nilotica, Acacia senegal, Acacia tortilis, Balanites aegyptiaca, Maerua crassifolia, Salvadora persica, and Ziziphus mauritiana.

Limited Distribution

4.2 General biophysical aspects of the Mékrou Area of Interest and Influence

4.2.1 *Digital Elevation Model, Slopes and Land Forms*

Before September 2014, a Digital Elevation Model known as SRTM90 was available at 3 arc-seconds or about 90 meters spatial resolution. This DEM comprises a combination of data from NASA´s Shuttle Radar Topography Mission and it´s provided by USGS EROS Data Centre. Afterwards, a higher spatial resolution DEM was released at 30m resolution [8]. Figure 10 shows a map with the latter from where slopes for the area of influence have been calculated (Figure 11). The Land Surface Forms data set (Figure 12) is available at the Geosciences and Environmental Change Science Centre (GECSC-USGS) website, and corresponds to one of the input data layers used to calculate the Global Ecological Land Units [7] (Figure 9).

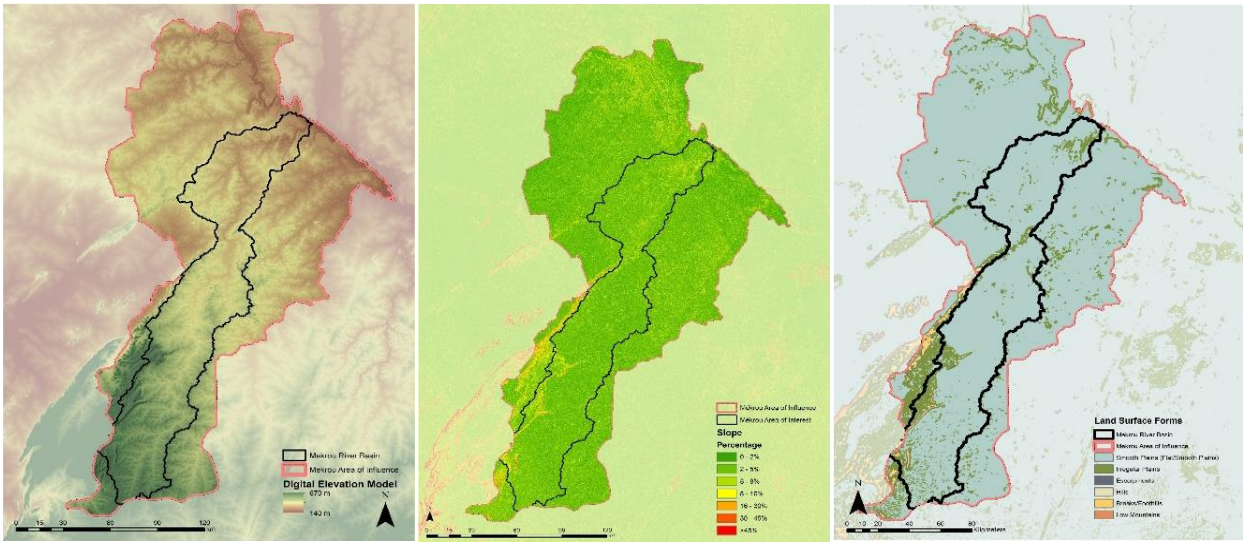

Figure 10. Digital Elevation Model Figure 11. Slope percentage Figure 12. Land Surface Forms

The highest altitudes can be found in the south-western hills of Kouandé commune with a maximum of about 670 meters, while the confluence zone between Mékrou and Niger River presents the lowest with 140 meters. Smooth or almost flat plains and low to moderate slopes are dominant throughout practically the whole territory with some zones with steeper slopes again in the mountainous south-western hills. Irregular plains with variable slopes can also be found spread, especially along the river and some other north-western areas. This characteristic makes possible to find waterfalls, gorges, and rapids along the 445km of the Mékrou River, which approximately starts at 400 meters of altitude in the communes of Kouandé and Péhunco and ends at about 160 meters (Figure 13).

In order to show an example of those abrupt changes figure 13 also shows, both, an altitudinal profile for the entire Mékrou River and a transversal profile example for altitudes and slopes located nearby the border of W-Park.

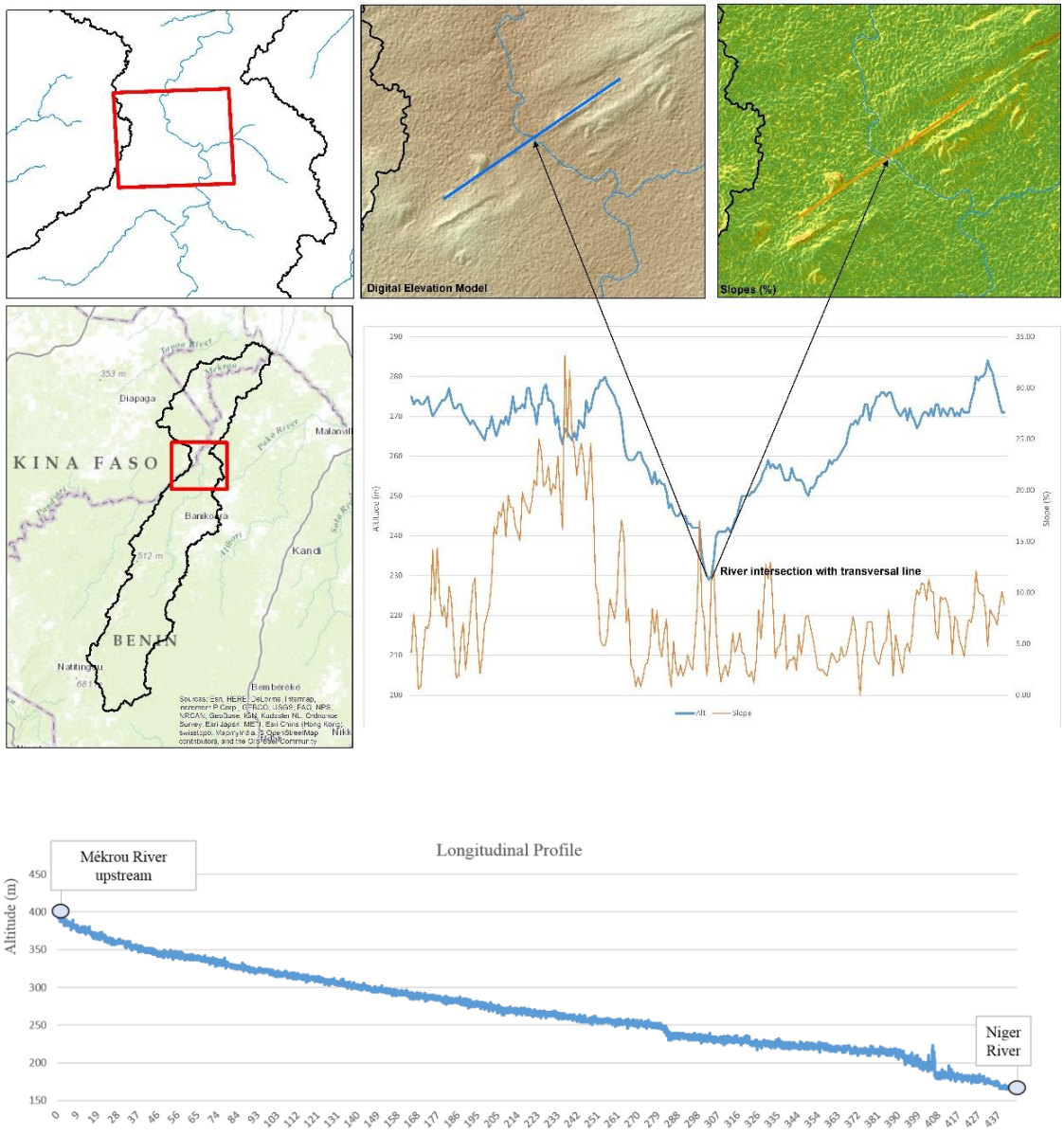

Figure 13. Longitudinal and transversal profiles for altitude and slopes (%)

4.2.2 *Hydrology*

4.2.2.1 River Network and Watersheds/Catchments

The HydroSHEDS dataset [10] is a mapping product that provides hydrographic information for regional and global-scale applications offering a suite of geo-referenced data sets at various scales, including, among others, river networks and basin and watersheds/catchments boundaries. It is based on elevation data obtained under the Space Shuttle flight for NASA's Shuttle Radar Topography Mission (SRTM90) [9]. Catchments and watersheds can be downloaded form the HydroBASINS website [11]. It provides hierarchical sub-basin breakdown representing a subset of the previous.

The River Network (Figure 14.a) is represented as a vector file that, according to the HydroSHEDS procedure, was derived from the drainage directions layer. Only rivers with upstream drainage areas exceeding a certain threshold were selected for the calculation: for the 15 arc-second resolution a threshold of 100 upstream cells was used. In this sense, the Mékrou River flows in south-north direction and shows a relatively simple network without any major tributaries.

Figure 14.b shows level 8 and 10 of the hierarchical sub-basin breakdown while the basin physical boundary corresponds to level 6. Level 8 is formed by 9 different catchments with an average area of 1175 km^2 (max. 2575km^2, min. 550km^2). Level 10 is formed by 74 smaller catchments with an average area of 142km2 (max. 288km^2, min. 2km^2).

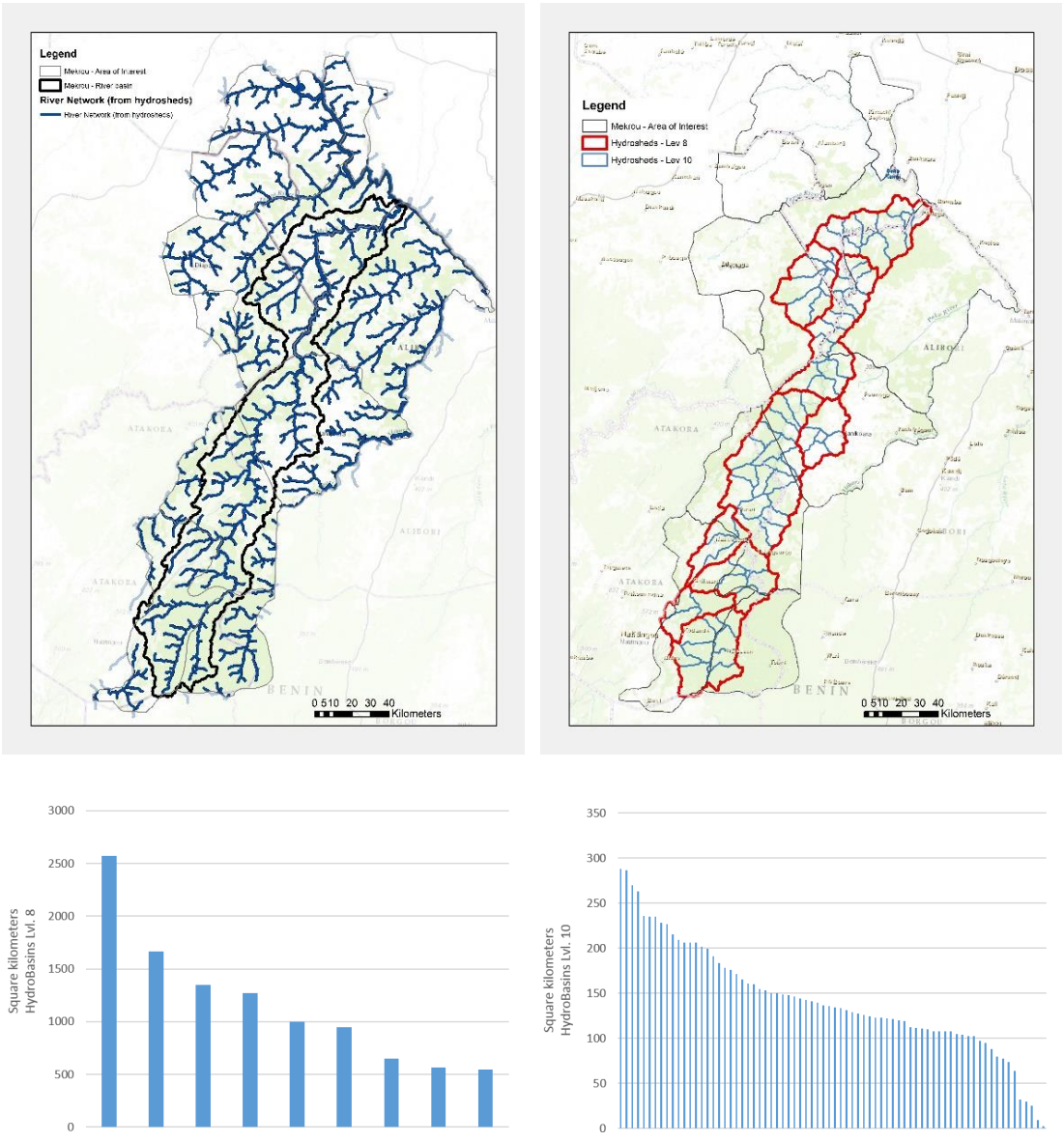

Figure 14. a) River Network and b) Catchments (HydroBasins) Graphs show the area of the catchments at level 8 and 10.

A simplified river network for Niger and Mékrou rivers was also derived from the DEM for modelling purposes (SWAT routines were used to derive it).

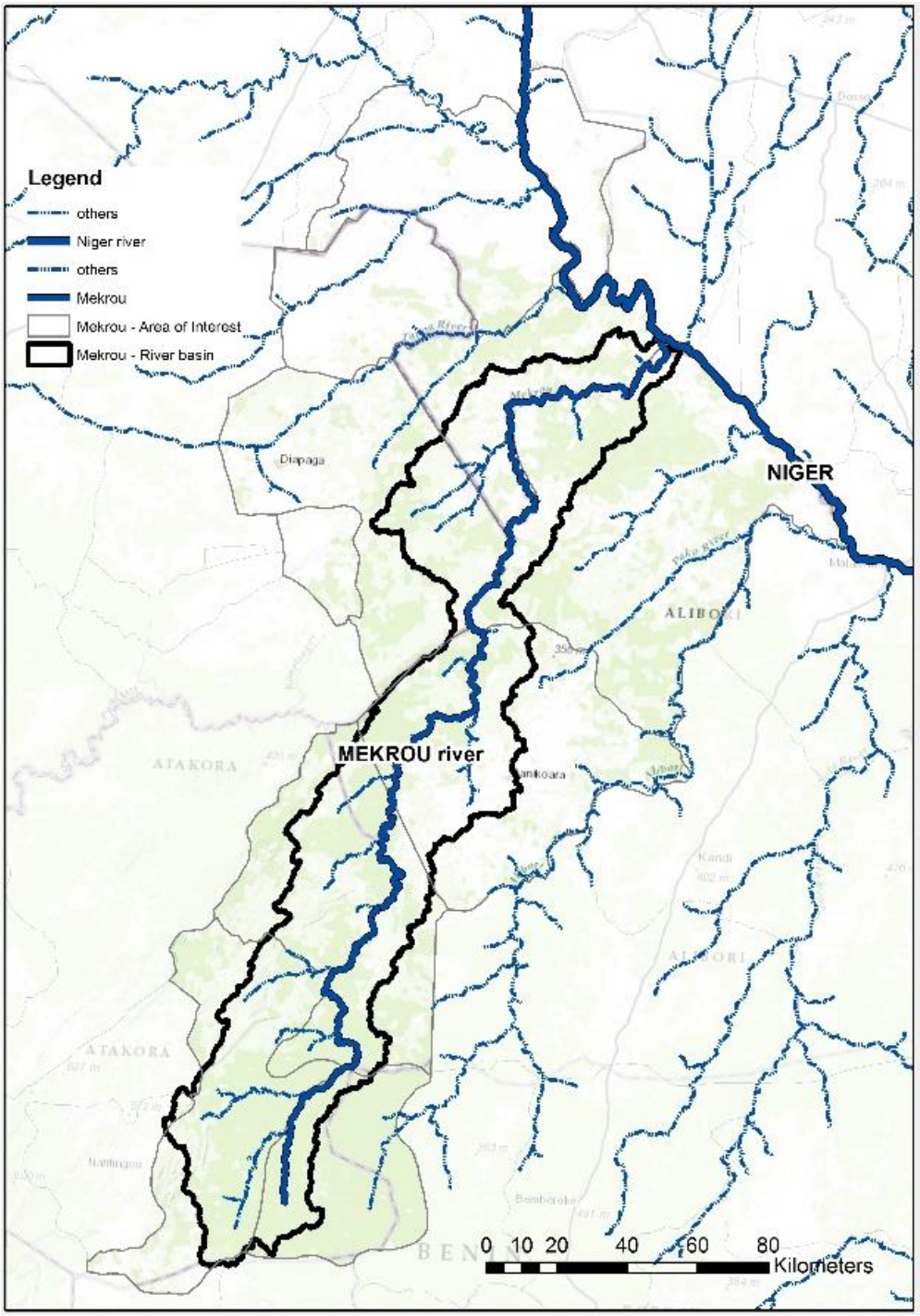

Figure 15. Simplified river network

4.2.3 *Precipitation, temperature and discharge regimes*

In line with the precipitation average values of the Sudano-Sahelian ecological zones, the basin average accumulated annual rainfall varies from 600mm near the confluence with the Niger River, to about 1200 mm in the upstream. Rainfall data from ground weather stations provided by national meteorological institutions participating in EUROCLIMA project [12] allow a relatively homogeneous spatial coverage around the study area. In this sense, 10 stations have been used to derive mean annual and monthly precipitation: five in the north: Birni-Ngaoure, Dioundiou, Gaya Nier, Say and Torodi, and other five in the south: Bembereke, Djougou, Kandi, Natitingou and Tanguieta. The time scale varies depending on the stations, starting in most cases in 1950 and ending in around 2000. Alternative data sources such as, for example, CHIRPS (Climate Hazards Group Infrared Precipitation with Station data [13]) (Figure 16) or other satellite derived products (TRMM, RFE, etc.) can also be used to better describe precipitation patterns [14] and complete the time series. However, rainfall station data serve as a first insight into general patterns and characterization of annual and monthly averages.

In general, rainfall in the basin shows high variability in time and space and follows a cyclical trend of wet and dry periods. The mean monthly precipitation for the wettest month in the southern and northern region varies between 200 mm and 300mm, respectively, being the driest (November-February) close to zero. The coefficient of variation (the standard deviation of the monthly precipitation estimates expressed as a percentage of the mean of those estimates) also shows a clear south-north pattern, which also reflects the different nature between the dry and the semi-arid regions commented before.

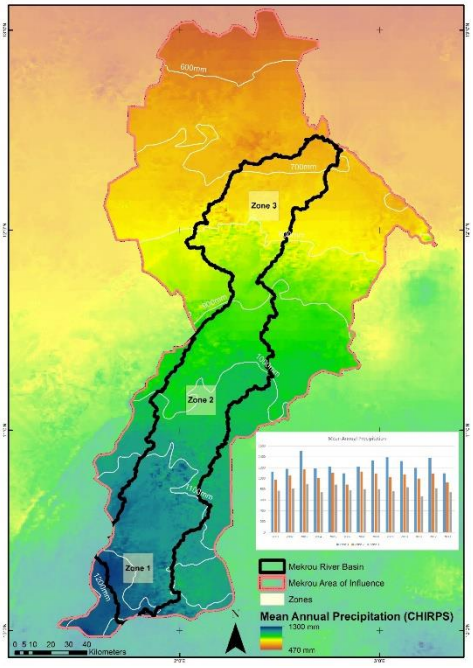

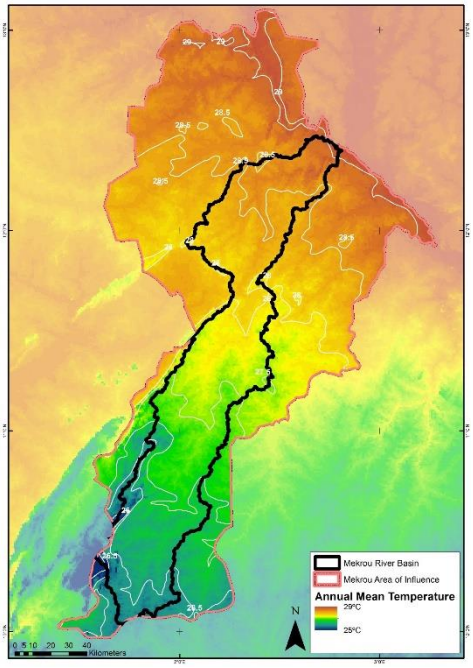

Figure 16. Mean Annual Precipitation Figure 17. Mean Annual Temperature

Mean annual temperature (Figure 17) ranges from almost 30ºC in the north to 26.5ºC in the south, being the warmest month April with a maximum temperature of 40ºC in the north and 35ºC in the south. The minimum temperature of the coldest month (September), is around 19ºC in the north and 15ºC in the south, leading to a lower annual range in the latter, being the semi-arid region the one that presents the highest values with about 25ºC of variation. The Temperature Annual Range is calculated as the difference between the maximum temperature of the warmest month and the minimum temperature of the coldest. The Mean Diurnal Range (Mean of monthly (max. temp – min temp)) varies between 14ºC in the north and 12.8ºC in the south. Mean annual temperature, temperature of warmest month (TWM), temperature of coldest month (TCM), temperature of annual range, precipitation of wettest month (PWD), precipitation of the driest month (PDM) and the coefficient of variation (Figures 19, 20, 21) have been derived from the Global Climate Datasets (WorldClim) [15].

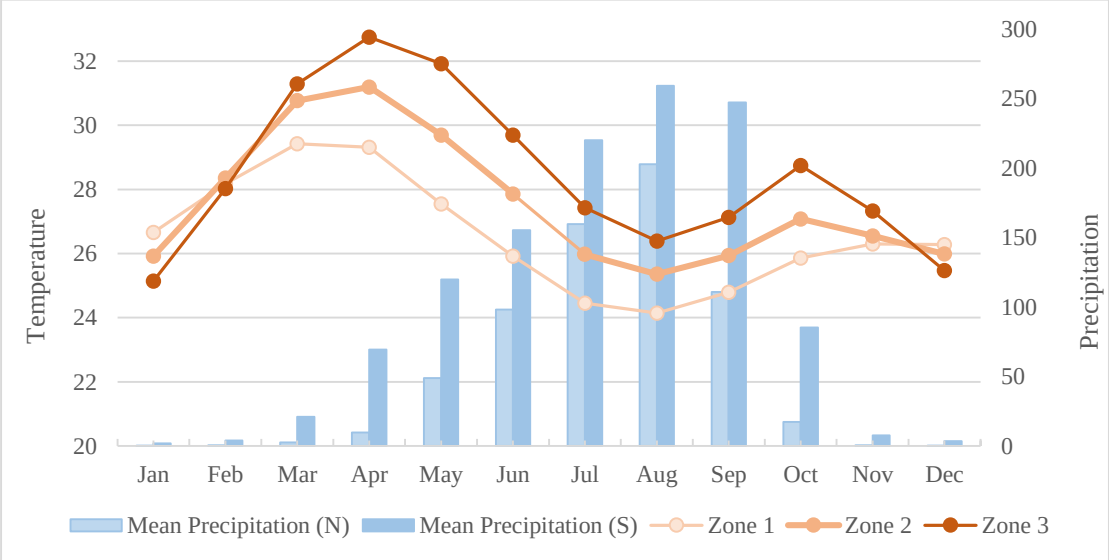

Figure 18. Mean monthly precipitation (CHIRPS) and temperatures (WorldClim database)

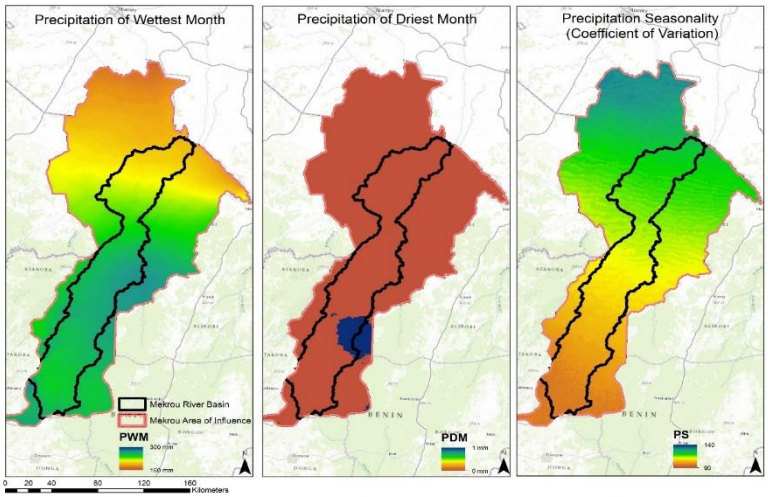

Figure 19. PWM, PDM, Seasonality Figure 20. TWM, MTCM, Annual Range

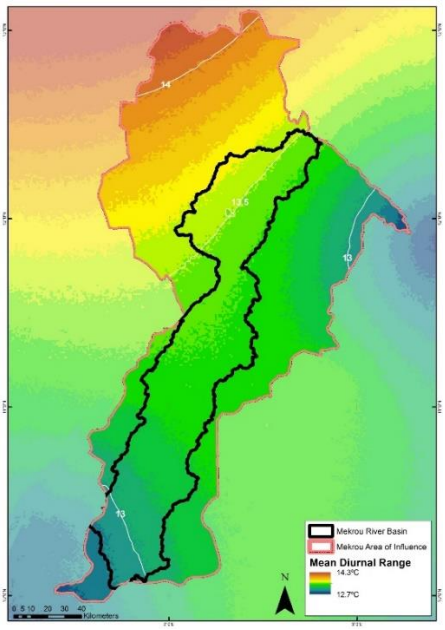

Figure 21. Mean Diurnal Range

Data series of observed historic discharge are available at JRC under a cooperation agreement between the Global Runoff Data Centre (GRDC) [16] and the Climate Risk Management and Water Units within the Institute for Environment and Sustainability. The available database comprises discharge data of more than 9200 gauging stations from all over the world over a period of several years that was supplemented with the *UNESCO monthly river discharge data collection 1965-85*.

Within the Mékrou basin, there is one station available with discharge data covering the period 1961-2010. Unfortunately, most of the time series has missing data, so only data ranging from 1961 to 1978 have been used to characterize average monthly discharges. Additionally, four nearby stations (Table 4) have been selected: three in the Niger River and an additional one in the Goroubi River, a basin located in the western region that shares similar characteristics with the Mékrou. In this sense, caution must be paid as considered years are within the very long drought period started in the 1970s and so with the subsequent strong decreases in the precipitation and discharge regimes. Considering this drawback, long-term discharge patterns cannot be detected with this times series and consequently caution must be also paid with water flow rates detected for example in the decade 1980-1990, that are the lowest recorded since the beginning of the century [20].

Name	River	Country	GRDC No	Lat.	Long.	Alt.	Catchment area	Next station Id	Units	Time series	Years
NIAMEY	Niger	NER	1234150	13.52	2.08	176	700000	1234250	m³/s	1929 - 2012	84
DIONGORE AMONT	Goroubi	NER	1234180	12.96	2.32	NA	15350	1234250	m³/s	1962 - 1988	27
W	Niger	NER	1234201	12.58	2.61	NA	NA	1734500	m³/s	1985 - 2009	25
BAROU	Mekrou	BAF	1734450	12.35	2.73	173	10500	1234250	m³/s	1961 - 2010	50
MALANVILLE	Niger	BAF	1734500	11.86	3.38	155	1000000	1835110	m³/s	1952 - 2000	49

Table 4. GRDC station characteristics around the Mékrou area of Influence.

Monthly Averages (discharge)	Jan.	Feb.	Mar.	Apr.	May.	Jun.	Jul.	Aug.	Sep.	Oct.	Nov.	Dec.
Goroubi river (Diongore Amont)	0.00	0.00	0.00	0.00	0.09	1.84	8.80	17.94	30.07	12.07	1.54	0.00
Mekrou river (Barou)	0.88	0.15	0.00	0.00	0.41	3.85	14.51	62.91	150.37	91.19	21.81	4.20
Niger River (W)	1223.37	818.04	382.57	147.62	67.07	64.91	147.39	441.22	880.20	1104.56	1264.65	1369.44
Niger River (Niamey)	1554.67	1332.68	928.41	498.17	195.43	83.19	145.29	574.12	1089.53	1244.85	1409.74	1561.54
Niger River (Malanville)	1487.78	1316.24	1028.07	624.97	262.32	134.56	208.39	843.29	1571.96	1508.99	1398.50	1484.21

Table 5. Monthly mean discharges for five stations within and around the Mékrou river basin.

The observations of discharge data (Table 5) are closely linked with local that strongly increases the flow precipitation (Figure 22), being this the major controlling factor with evaporation and infiltration effects being of secondary importance. Barou station shows that the flood of the Mékrou river lasts from July to November being the peak in September with around 150m^3/s, and the low-water period occurs from December to June. The Goroubi River shows a similar pattern but with lower flow rates while the Niger River, as it receives tributaries from different areas, increases also it´s flow around August, maintaining this regime until around January when it starts decreasing until June. In this sense, the discharge in Niger River has a dual behaviour that is mainly affected by the tributaries of the Sahelian regime and the upper tropical transition regimes.

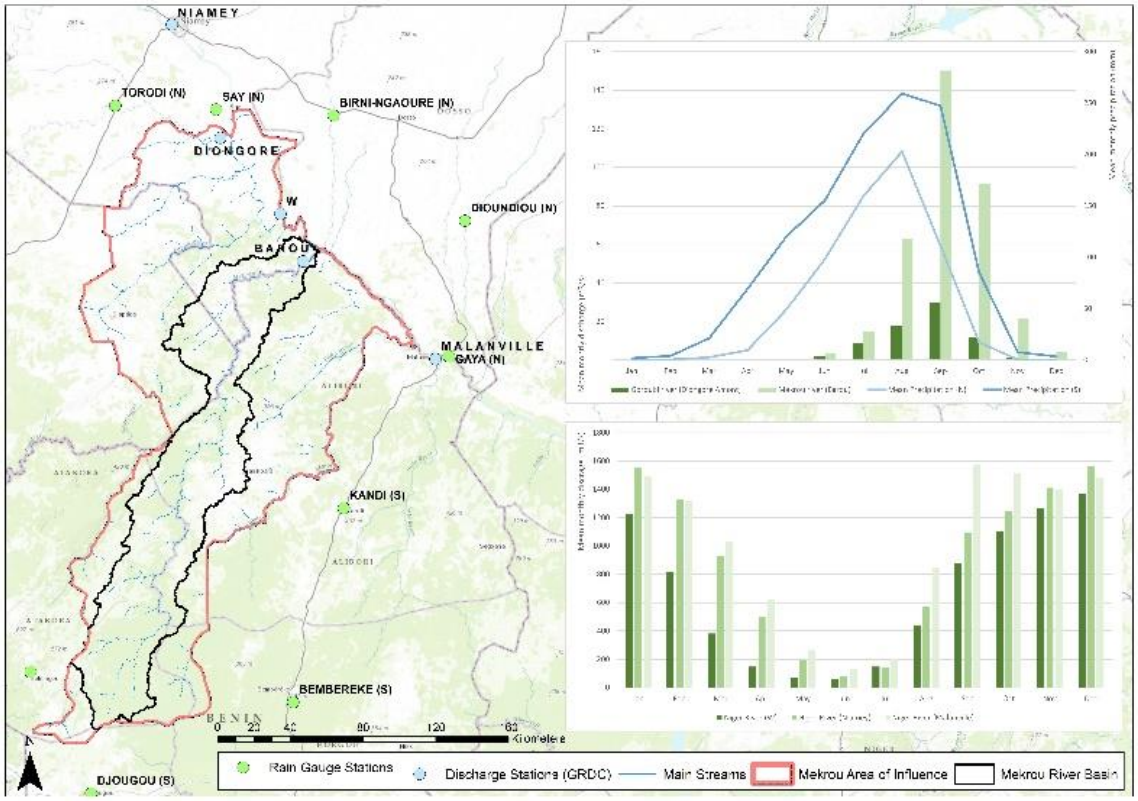

Figure 22. Mean monthly precipitation and discharge

4.2.4 *Evapotranspiration and Aridity Index*

MOD16 Global Evapotranspiration data set is part of NASA/EOS project to estimate global terrestrial evapotranspiration from earth land surface by using satellite remote sensing data. This product can be used to calculate regional water and energy balance, soil water status; hence, it provides key information for water resource management. With long term ET data, the effects of changes in land use, and ecosystem disturbances on regional water resources and land surface energy can be quantified.

MOD16 can be accessed through the Numerical Terradynamic Simulation Group website (University of Montana) [17] where different products are available, such as, for example MOD16 global evapotranspiration (ET)/latent heat flux (LE)/potential ET (PET)/potential LE (PLE) 1km^2 grids at 8-day, monthly and annual intervals. The dataset covers the time period 2000 – 2010.

In the other hand, the Global Aridity Index (Global-Aridity) dataset (Figure 25) it's expressed as a generalized function of precipitation, temperature, and/or potential evapotranspiration (PET) and it's related to rainfall deficit for potential vegetative growth [18]. The mean Aridity index is calculated from the 1950-2000 period at 30 arc-second spatial resolution and is calculated as:

$$\underline{\text{Aridity Index (AI)}} = \text{MAP/MAE}$$

Where: MAP = Mean Annual Precipitation and MAE / Mean Annual Potential Evapot-Transpiration.

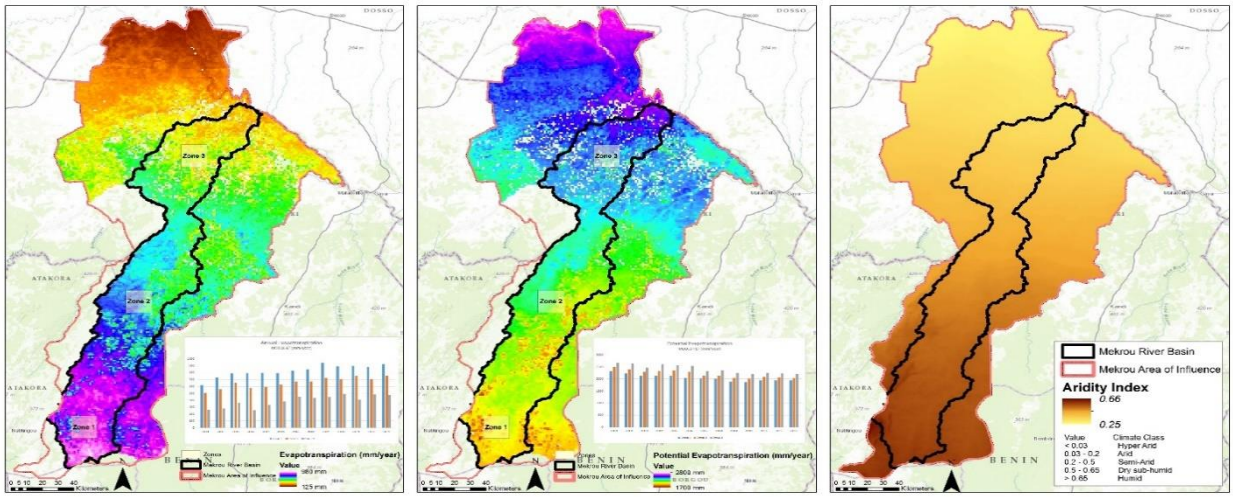

Figure 23. Evapotranspiration Figure 24. Potential Evapotranspiration Figure 25. Aridity Index

http://www.cgiar-csi.org/data/global-aridity-and-pet-database#description

Note that higher values and darker colours represent more humid conditions, with low AI and lighter colours representing higher aridity. Following the generalized climate classification scheme for Global aridity values [19], the southern part can be defined as dry sub-humid (0.5-0.65) class, being some very few values above 0.65 (humid class). Conversely, the north is characterized by lower precipitation rates and higher temperatures and PET values, and so the area is classified as semi-arid with AI values are between 0.2-0.5.

AI value	Climate Class
<0.03	Hyper Arid
0.03 - 0.2	Arid
0.2 - 0.5	Semi-Arid
0.5 - 0.65	Dry sub-humid
> 0.65	Humid

Table 6. Climate classification scheme for Global aridity values.

Regarding evapotranspiration (Figure 23), the mean maximum annual evapotranspiration values can be found in the southern part, being around 900 mm/year, while the minimum values correspond to the northern with around 400mm/year. Monthly evolution of ET shows a pattern related to precipitation (Figure 26) and with mean NDVI values for the three studied zones within the basin.

Conversely and in line with the Aridity Index, the ETP (Figure 24) follows a south-north pattern, with lower values in the south and higher in the north. The ETmax and ETPmin occur in September, when the precipitation and temperature are maximum, as well as the NDVI values. More details related to the Normalized Difference Vegetation Index as well as available data sources for its calculation is given within the Land Cover section.

Limited Distribution

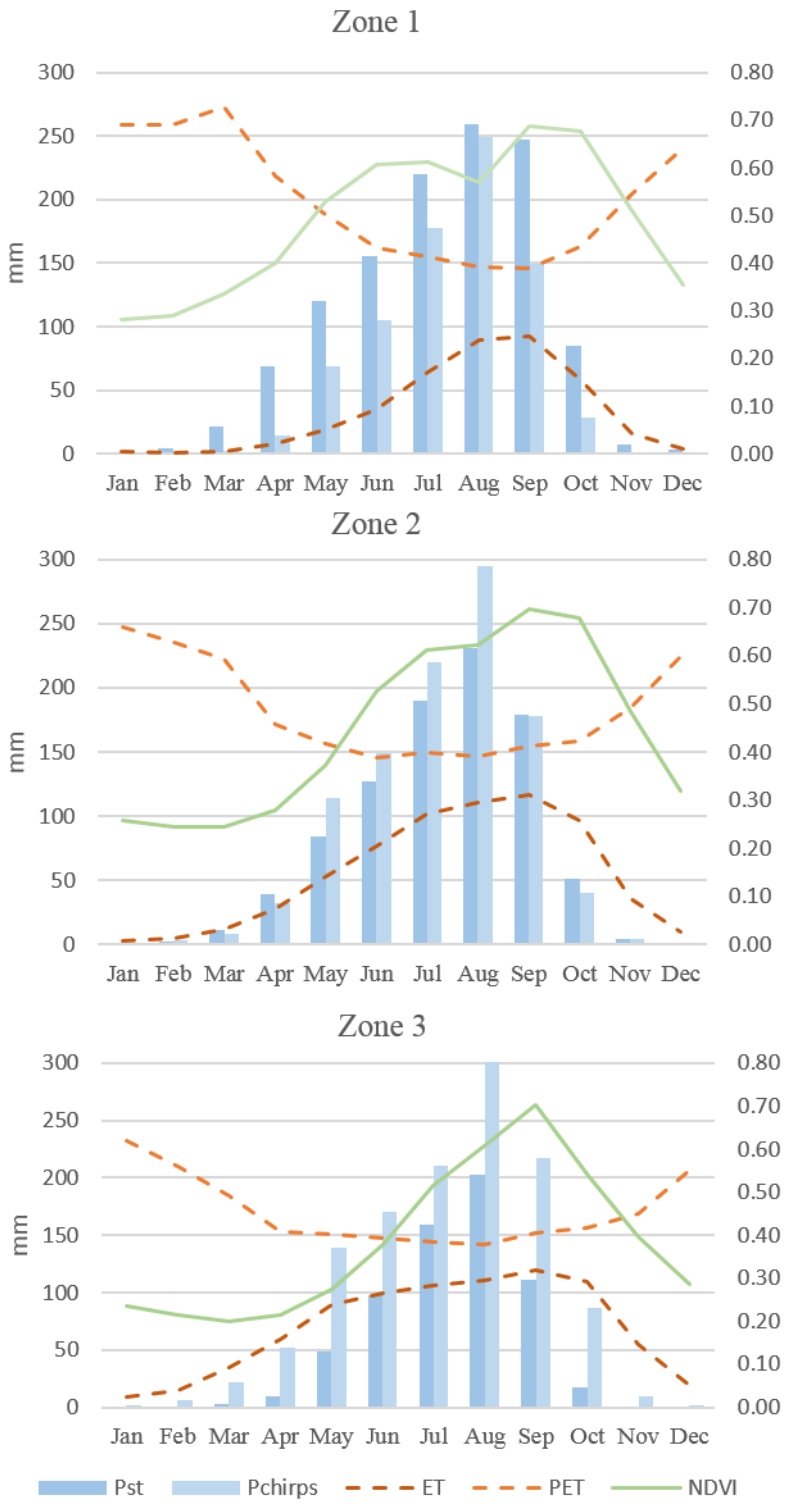

Figure 26. Precipitation (rain gauge stations vs. CHIRPS), Evapotranspiration (ET), Evapotranspiration (ETP) and NDVI mean monthly evolution.

4.2.5 *Geology*

4.2.5.1 Lithology and Lineaments (faults, cracks, folds)

The GLiM database [21] is the one with the highest detail on lithological information in the region. At global scale, the GLiM identifies 16 lithological classes at its most general level of classification. According to the information therein (Figure 27), metamorphic rocks cover the largest part of the area of interest, while in the northern and north-eastern part there are also some siliciclastic sedimentary formations.

Information regarding lineaments (Figure 29) is available so far, only for the Burkina Faso part of the catchment, digitised from the 1976 Geological map, published by the Directorate of Geology and Mines. According to that map, there are two thrust faults in the area, one fault and three probable faults.

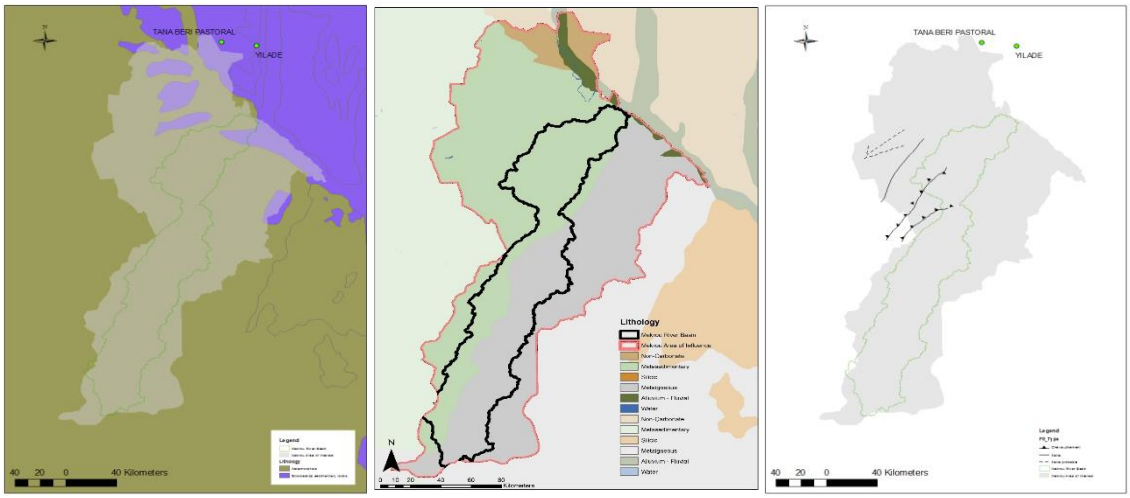

Figure 27. Lithology Figure 28. Lithology II Figure 29. Lineaments (faults, cracks, folds)

4.2.6 *Hydrogeology*

4.2.6.1 Groundwater distribution

From the results of the global model that has been developed [22], a map of the region can be obtained showing the simulated groundwater table depth (Table 7) for the whole region. Since there were no calibration points within the area of interest, it is possible that the simulation data will have discrepancies with the actual situation. Nevertheless, the simulated results can give a first educated guess of the expected situation in the field, since the model takes into account multiple parameters of the water cycle. The groundwater distribution (Figure 30) is calculated as the difference between the land surface at each point and the respective water table depth value.

	COUNTRY	NAME	NAME	MIN [m]	MAX [m]	MEAN [m]	STD [m]	RANGE [m]
1	Niger	Tillabéry	Kollo (Kirtachi)	140.1	220.8	191.5	11.9	80.7
2	Niger	Tillabéry	Say	136.2	269.3	214.8	23.6	133.1
3	Burkina Faso	Tapoa	Bottou (Botou)	191.3	259.1	232.4	12.2	67.8
4	Burkina Faso	Tapoa	Diapaga	176.1	322.3	254.5	17.9	146.2
5	Burkina Faso	Tapoa	Tansarga	199.0	319.3	254.1	27.2	120.3
6	Benin	Alibori	Banikoara	211.3	379.5	272.7	20.8	168.2
7	Benin	Alibori	Karimama	131.0	298.2	220.6	27.9	167.2
8	Benin	Atakora	Kérou	123.1	473.8	323.4	48.0	350.8
9	Benin	Atakora	Kouandé	270.2	623.3	400.9	54.1	353.1
10	Benin	Atakora	Péhunco (Pehonko)	294.5	436.7	358.4	26.8	142.3
			Average	187.3	360.2	272.3	27.0	173.0

Table 7. Statistical analysis results of simulated water table values from (Fan et al., 2013)

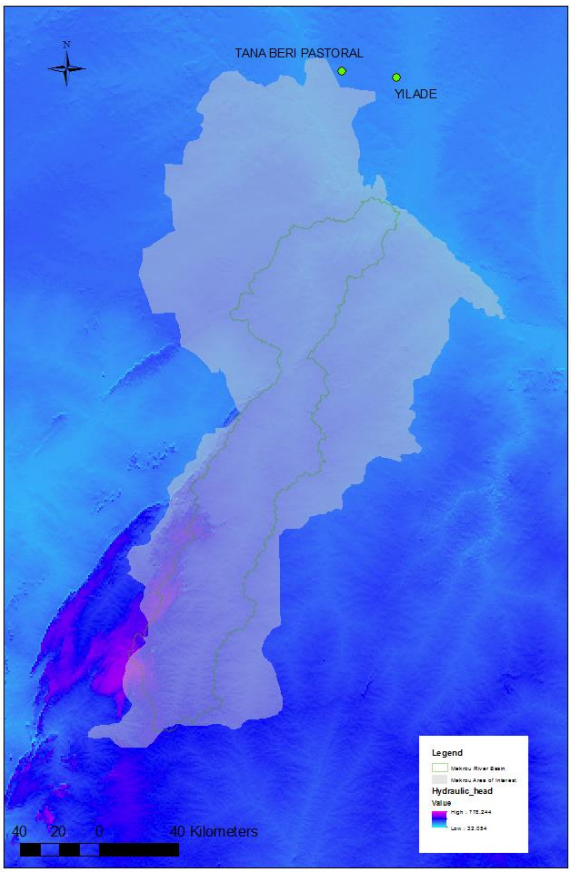

Figure 30. Groundwater distribution

4.2.6.2 **Depth to the water table**

A direct output of the aforementioned global model [22] was the simulated depth to the water table (Table 8, Figure 31). The data are available for download from the journal's website.

	COUNTRY	NAME	NAME	MIN [m]	MAX [m]	MEAN [m]	STD [m]
1	Niger	Tillabéry	Kollo (Kirtachi)	0	63.9	31.7	14.3
2	Niger	Tillabéry	Say (Parc W)	0	51.3	16.9	11.9
3	Niger	Tillabéry	Say (Tamou)	0	56.6	23.9	13.6
4	Burkina Faso	Tapoa	Bottou (Botou)	0	39.1	13.8	9.0
5	Burkina Faso	Tapoa	Diapaga	0	86.4	13.0	10.8
6	Burkina Faso	Tapoa	Tansarga	0	52.0	9.8	11.1
7	Benin	Alibori	Banikoara	0	86.2	12.4	10.5
8	Benin	Alibori	Karimama	0	66.2	14.2	11.2
9	Benin	Atakora	Kérou	0	119.9	13.8	14.0
10	Benin	Atakora	Kouandé	0	113.4	17.0	16.0
11	Benin	Atakora	Péhunco (Pehonko)	0	55.1	13.7	10.3
			Average	0	71.8	16.4	12.1

Table 8. Statistical analysis results of simulated water table depth values from (Fan et al., 2013)

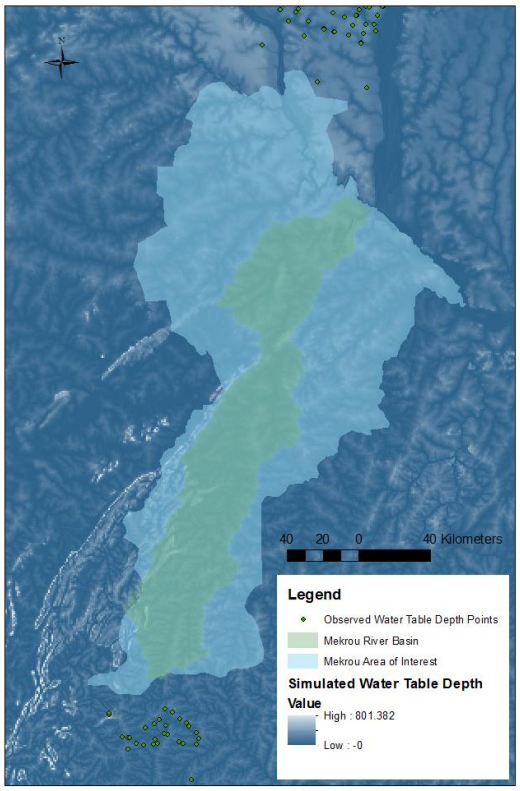

Figure 31. Depth to the water table

4.2.7 *Soils*

The Harmonized World Soil Database [23] with a resolution of about 1 km was used to characterize soils in the Region.

Different soil data are available for each soil mapping unit and soil typology and for 2 soil layers. Data are stored in a Geodb (ex: data: texture, drainage, AWC, soil depth, organic carbon, gravel, bulk density, CaCO3, TSB, etc).

Data at 6 reference depths (2.5,10,22.5,45,80,150 cm) are also available as 1km raster grid (Hengl T. et al. 2014) containing spatial modelled data for a selection of soil properties soil organic carbon (g kg−1), soil pH, sand, silt and clay fractions (%), bulk density (kg m−3), cation-exchange capacity (cmol+/kg), coarse fragments (%), soil organic carbon stock (t ha−1), depth to bedrock (cm), World Reference Base soil groups, and USDA Soil Taxonomy suborders.

4.2.7.1 **Soil Type**

A total of 16 different soil mapping units corresponding to 6 different soil types are available in the region of interest (Figure 32) [26, 27].

Dominant soil in the area are classified as Ferric Luvisols (58% of the area). The Reference Soil Group of the Luvisols holds soils whose dominant characteristic is a marked textural differentiation within the soil profile, with the surface horizon being depleted of clay and accumulation of clay in a subsurface ‘argic’ horizon.

Other dominant soil types are Eutric Regosols (17%) and Lithosols (12%).

Regosols are very weakly developed mineral soils in unconsolidated materials that have only an ochric surface horizon and that are not very shallow. Regosols are extensive in eroding lands, in particular in arid and semi-arid areas and in mountain regions.

Lithosols may be described as soils which are shallow or stony: usually there is a limiting horizon of consolidate rock or massive material.

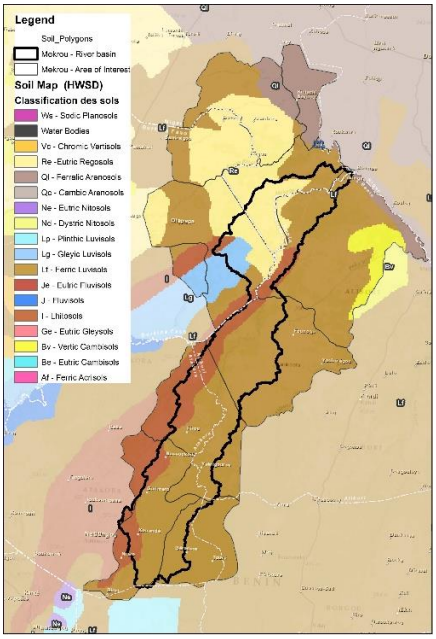

Figure 32. Soil Types

Limited Distribution

4.2.7.2 **Soil Top Layer organic carbon content**

Organic carbon content ranges between very low values (about 0.3 %) to moderate values (1 – 1.4%) (Figure 33).

Average organic carbon content in the area is about 0.8 % which is a quite limited value to support a high productive agriculture (above all on the long term).

Anyway this data are derived from a limited number of survey and maybe more local data would show a better discretization of soil and would allow to identify richer regions in organic carbon and potentially more productive. The richest soils for the organic carbon content are the lithosols and are located in the western part of the River basin.

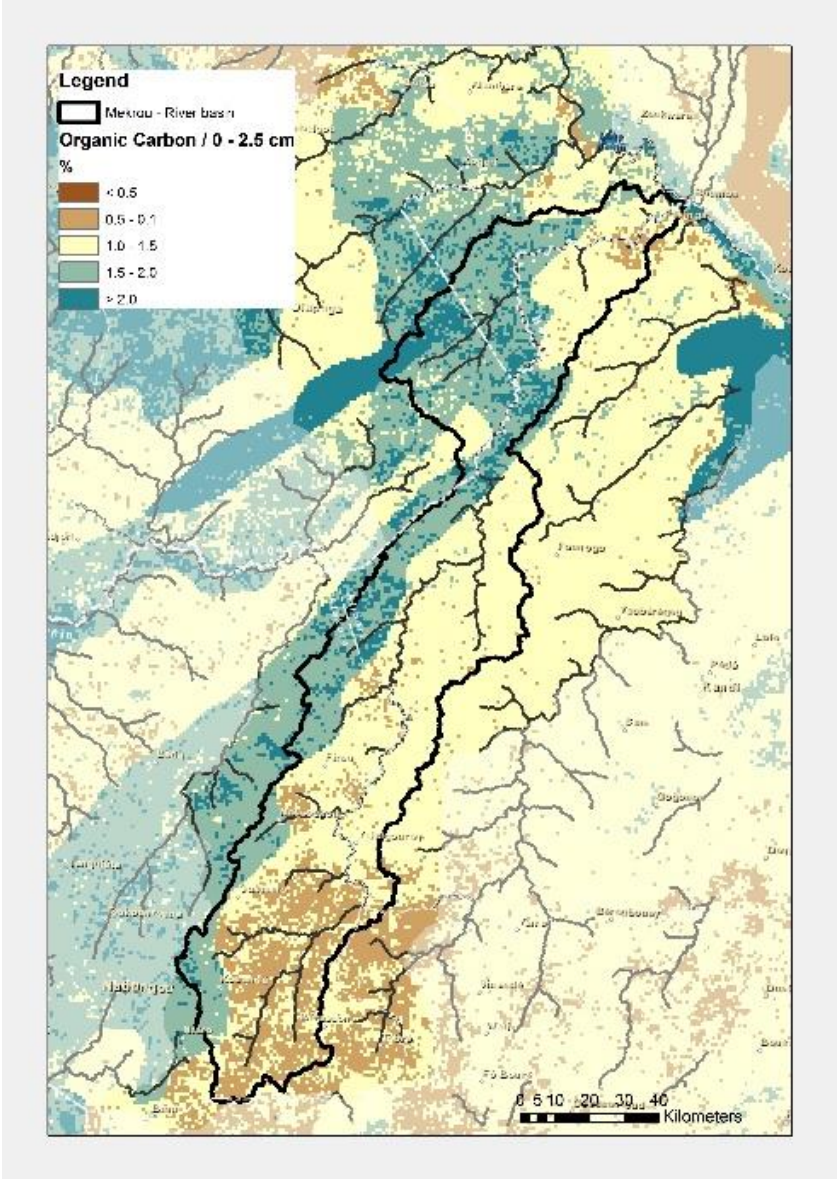

Figure 33. Soil Top layer Organic Carbon content

4.2.7.3 **Soil Top Layer Texture class**

Soil texture is a qualitative classification tool used in both the field and laboratory to determine classes for agricultural soils based on their physical texture. The class is then used to determine crop suitability and to approximate the soils responses to environmental and management conditions such as drought.

In the area the dominants texture classes are the sandy-clay-loam and loam which corresponds to intermediate classes (Figure 34). In general high content of sand (>85%) limits agricultural suitability: also high content of clay (>50%) and Lime (>60%) may limit soil suitability for crop production. In the basin soil with the highest content of sand are mainly located in the Northern eastern part, while in the central and in the south the sand content is quite moderate (See Sand Content Map).

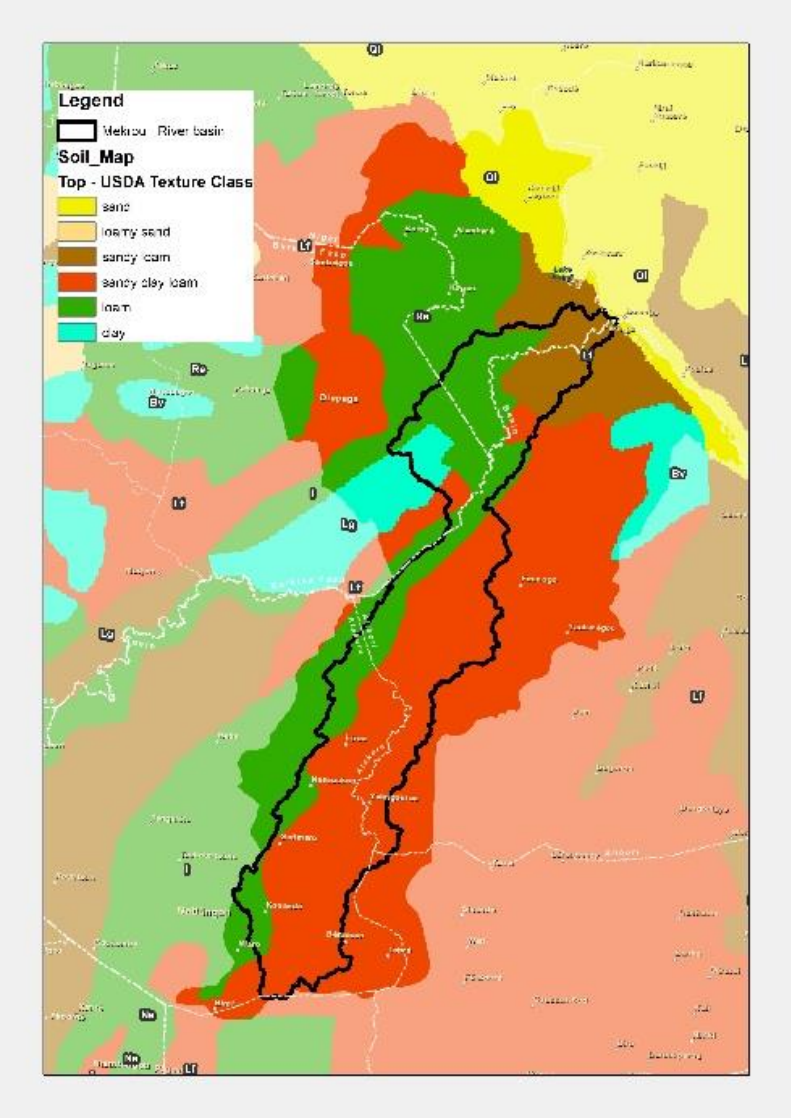

Figure 34. Soil Top layer Texture Class (for dominat soils)

4.2.8 *Landcover, deforestation and greenness seasonality*

There are currently several satellite-derived global land cover products available at different spatiotemporal scales and classification schemes (i.e. Global Land Cover 2000, GlobCover 2009, MODIS-LC, Globland30, UMD Land Cover). The lack of uniformity among the products, as well as associated uncertainties lead to an inconsistency when comparing them in a certain study area and makes difficult to determine a procedure to study specific patterns and analyse changes over time.

An alternative approach to enhance and better describe LC and its changes lies in carrying out self-classifications of multispectral satellite images (i.e. Landsat series, Sentinel-2, etc.) by applying pixel-based methods, object oriented approaches, decision tree classification algorithms and class thresholds, etc. However, a number of requirements should be considered in order to apply such a methodology at local or regional scale and obtain meaningful and accurate results. At the moment, the major drawback in the Mékrou area is the lack of ground-truth data to, for example, train the classification algorithms or obtain tailored class thresholds and conduct accuracy assessments.

Despite these limitations, some of these products or a mixture of them can serve as a first approach to understand the general composition of the different classes that conform the study area. In this sense, three products have been selected i) the Globcover regional product known as Africover, ii) Globeland30 and iii) Hansen2015 deforestation data sets. Additionally a spectral-unmixing analysis have been carried out in order to check the general consistency of the previous. NDVI temporal evolution derived from SPOT vegetation have also been used to get an idea on patterns related to vegetation seasonality.

4.2.8.1 **Land Cover**

The Global Land Cover Network (GLCN) as part of its activities has promoted the re-processing of the Globcover archive at national extent for the entire African continent. Globcover is an ESA initiative which began in 2005 in partnership with JRC, EEA, FAO, UNEP, GOFC-GOLD and IGBP. The aim of the project was to develop a service capable of delivering global composites and land cover maps using as input observations from the 300m MERIS sensor on board the ENVISAT satellite mission (http://due.esrin.esa.int/page_globcover.php)

The resulted data sets are vector based layers, coded using Land Cover Classification System (LCCS). This classification scheme is one of such system that has standardized classes with well-stablished definitions and thresholds [24, 25]

The data and associated metadata are published on the FAO´s Geonetwork catalogue. [xxx add link 1: http://www.glcn.org/databases/lc_gc-africa_en.jsp 2: http://www.fao.org/geonetwork/srv/en/main.home]

Considering the spatial resolution limitations of the previous product and taking into account that the entire Landsat archive was made freely available by the USGS, the development of GLC products at 30m resolution has become feasible. GlobeLand30 was produced by the National Geomatics Center of China and provides a 30 meter resolution data product with 10 LC classes for years 2000 and 2010 (within four years period) [28]. It does not follow the LCCS schema, but consists of 10 land cover types

that might be useful to study the general composition and main characteristics of the study area.

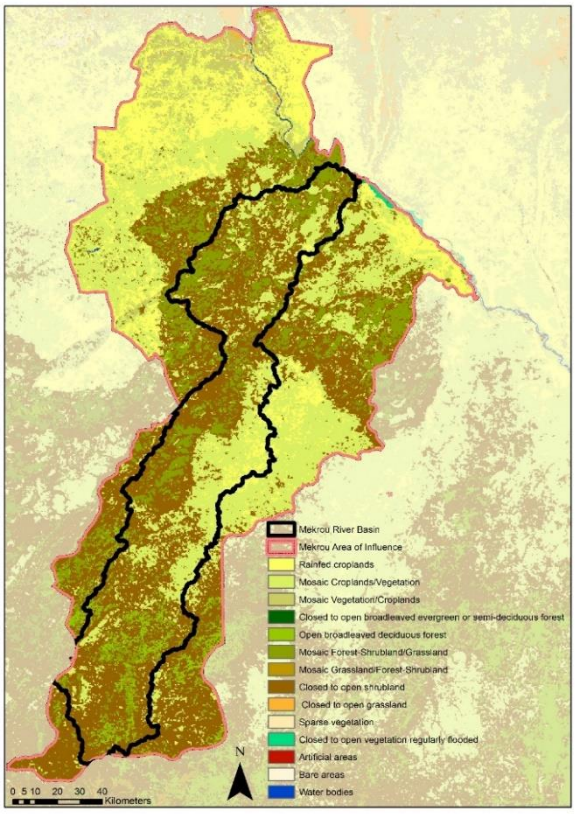

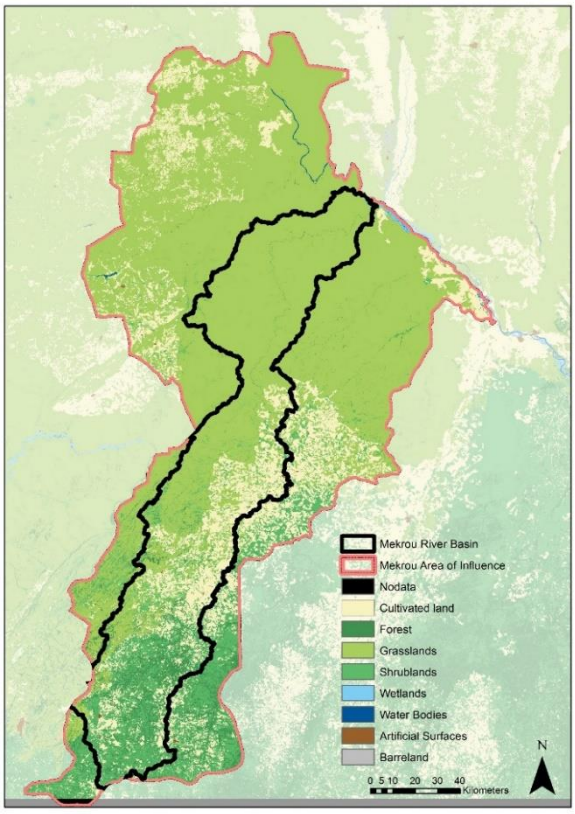

Figure 35. Land Cover 2005 (GLCN – Globcover Regional) Figure 36. GlobeLand30-2010

Despite the different classification schemas and class definitions, both products (Figure 35, 36) show similar covers throughout the study area. Looking at Globcover product, it can be seen that the area of interest is mainly formed by closed to open shrublands, followed by mosaic croplands/vegetation, mosaic forests and open deciduous forests, thus showing a high percentage of natural vegetation cover (Table 10). Similar areas can be found looking at the GlobeLand product, for which the main classes are grasslands, cultivated lands, shrublands and forests (Table 9).

Legend	GridCode	A-AOInt	A-AOInf
Cultivated land	10	199807	556824
Forest	20	81427	150835
Grassland	30	600147	2061808
Shrublands	40	177146	416157
Wetlands	50	546	7454
Water Bodies	60	183	6457
Artificial Surfaces	80	1047	2188
Barreland	90	3	136

Table 9. Land cover area – Globeland30 (Ha.) (Area of Interest and Area of Influence)

It should be considered that since the Globcover product presents more disagregated classes, cultivated lands in GlobeLand are probably represented as the sum of rainfed and mosaic croplands. Within the area of interest, these are mainly located in the region of Banikoara followed by Kérou, Kouandé and Péhunco (Benin). Agriculture development pressures over the limits of the W-Park as it can be visualy interpreted looking at the south-eastern border where the Mékrou river as well as the biodiversity conservation initiatives within the national park stop it´s development beyond these limits. Diapaga in Burkina Faso, Parc W in Niger and Karimama in Benin form part of the National Park where natural vegetation is the predominant class.

With lower agricultural development, mixed classes of shrubs and forested areas can be mainly found in the southern regions of Kouandé and Péhunco with some dissemianted patches in Kérou.

Legend	GridCode	A-AOInt	A-AOInf
Rainfed croplands	14	20910	398117
Mosaic Croplands/Vegetation	20	221504	799121
Mosaic Vegetation/Croplands	30	1535	193913
Closed to open broadleaved evergreen or semi-deciduous forest	40	0	23
Open broadleaved deciduous forest	60	112510	196476
Mosaic Forest - Shrubland/Grassland	110	135331	291597
Mosaic Grassland/Forest - Shrubland	120	1262	1765
Closed to open shrubland	130	566757	1300944
Closed to open grassland	140	0	159
Open grassland	143	0	2353
Sparse vegetation	150	0	9458
Closed to open vegetation regularly flooded	180	0	4373
Bare areas	200	331	1076
Water Bodies	210	88	7712

Table 10. Land cover area - Africover (Ha.) (Area of Interest and Area of Influence)

Closely linked to agriculture, logging and cattle activities, deforestation rates have increased during the last decade leading to an expansion of agricultural lands or croplands. Preliminary spatial analysis approaches can help to better understand the geographic patterns and main drivers behind this phenomenom as well as to measure the magnitude of changes occurred through time. For instance, clustering or hotspot analysis can be run to enhance the comprenhesion about where the socio-economical activity is concentrated within the basin, which are the barriers that affect it´s expansion or the impacts that are caused. Posterior analysis can also be carried out in order to understand associated factors such as the presence of roads, market accessibility, closeness to the water resource, etc. The following section tackles preliminarly some of these questions and gives an overview on defforestation rates between 2000 and 2014.

4.2.8.2 **Deforestation**

Hansen2015 product [29] have been used to analyse deforestation/afforestation extent and patterns between 2000 and 2014. This product, produced by the University of Maryland is based on Landsat time series (30m resolution) for trees defined as vegetation taller than 5 meters in height. The following are the data sets used to evaluate the incidence of deforestation/afforestation:

- Forest Cover Loss: defined as a stand-replacement disturbance or a change from a forest to non-forest state during the period 2000-2014. Forest loss is also given provided as 'Forest Loss Year', a disaggregation of total 'Forest Loss' to annual time scales.
- Forest Cover Gain: defined as the inverse of loss, or a non-forest to forest change entirely within the period 2000-2012.
- Tree Canopy cover for year 2000: defined as canopy closure for all vegetation taller than 5m height and is encoded as a percentage per output grid cell, in the range of 0-100.
- Reference composite cloud-free Landsat images are also provided for years 2000 and 2014.

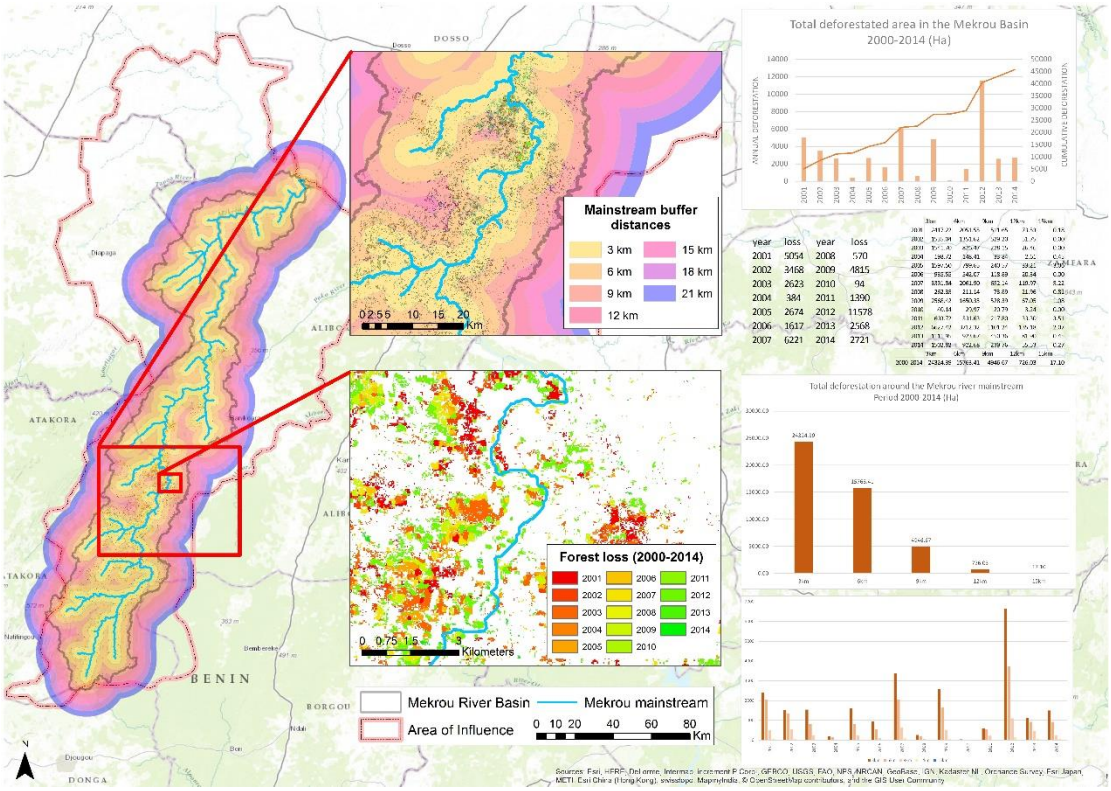

Figure 37. Gross forest cover loss 2000-2014

While afforestation (forest cover gain) is not detected within the area of interest, annual rates of deforestation over the different years show an irregular pattern (Figure 37). 2012 presents the highest values with approximatelly 11500 ha.s while the lowest happened during 2004, 2008 and 2010. The overall amount or cummulated deforested area between 2000 and 2014 is about 45000 ha.s. A first look at it´s spatial distribution

was carried out on the basis of a multiple ring buffer at 3 km distances around the Mékrou mainstream. The analysis shows at first glance that the closeness to the mainstream, thus, distance to the water resource is probably one of the drivers behind the deforestaion in the studied period. In the first 3 km. the total amount rises up to 24000 ha.s. being the area where more forest was cleared. In the following 3 kilometers (3 to 6 km) the area decreases to 15763 ha.s while the following (6 to 15 km) sum a total of 5689 hectares. This pattern is repeated for every single year. Should be also taken into account that these numbers might vary if we consider a longer time period, as some areas close to Banikoara were already deforested before 2000. Should be also highlighted that practically the majority of deforestation is concentrated in the non-protected areas, outside the borders of the W-National Park. Image on the left of figure 38 shows the deforestation percentages per square kilometer and it can be clearly seen that the border of the National Park as well as the Mékrou river act as a barrier that stops clearing beyond these limits. Only the hunting zone in Atakora (IUCN category VI) presents some clearings.

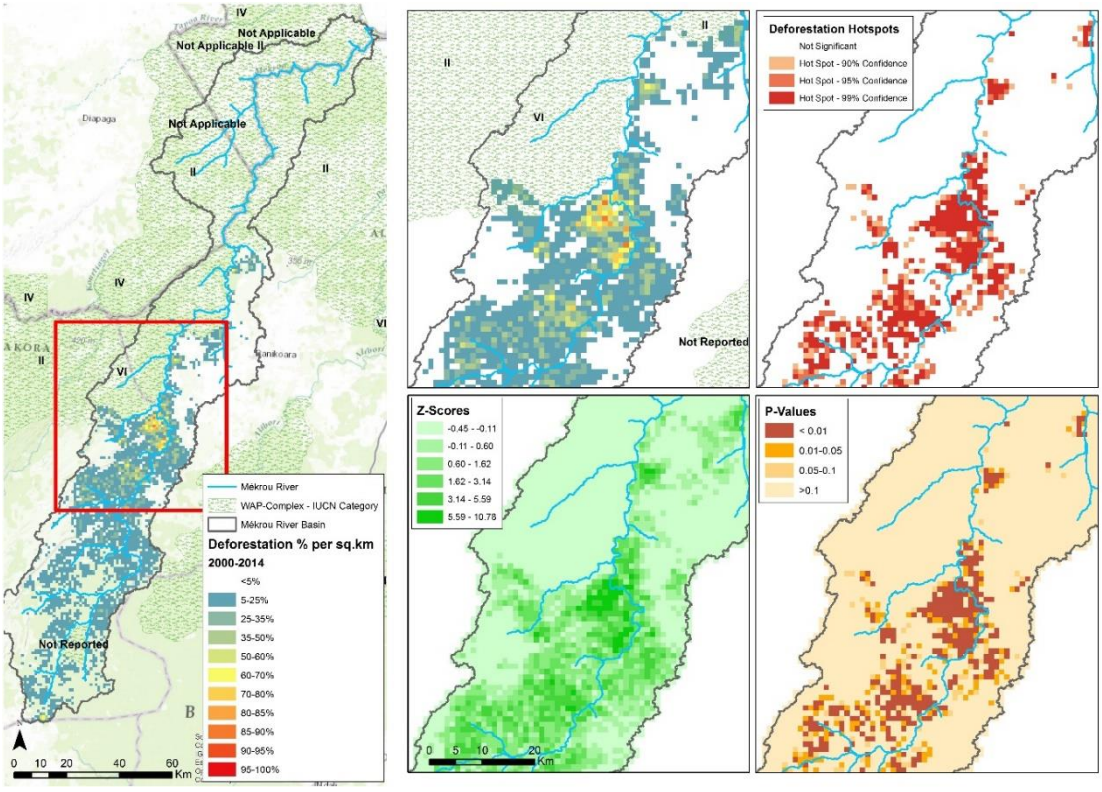

Figure 38. Deforestation Clustering - Hotspots

The hotspots analysis (Getis-Ord Gi*) shows that there is a higher concentration of deforestation in the Banikoara province but is also affecting some southern regions where there are yet wide forested areas as it can be seen in the Land Cover maps. Further analysis could help to improve the surveillance of these areas could give some insights about the underlying causes of deforestation and its persistence in these or other new spots.

4.2.8.3 **Spectral Unmixing**

In addition to the deforestation analysis and in order to support and/or check previous findings a linear mixture analysis was also carried out. This assumes that the signal received at the satellite depends on the proportion of soil, water and vegetation present in a particular pixel and on the mixing process. The Linear Mixture Analysis decomposes a mixed pixel into a collection of fractional abundances that indicate the proportions of vegetation, soil and water. The contribution of each pixel is assigned in proportion to the percentage area each ground cover class occupies in that mixed pixel.

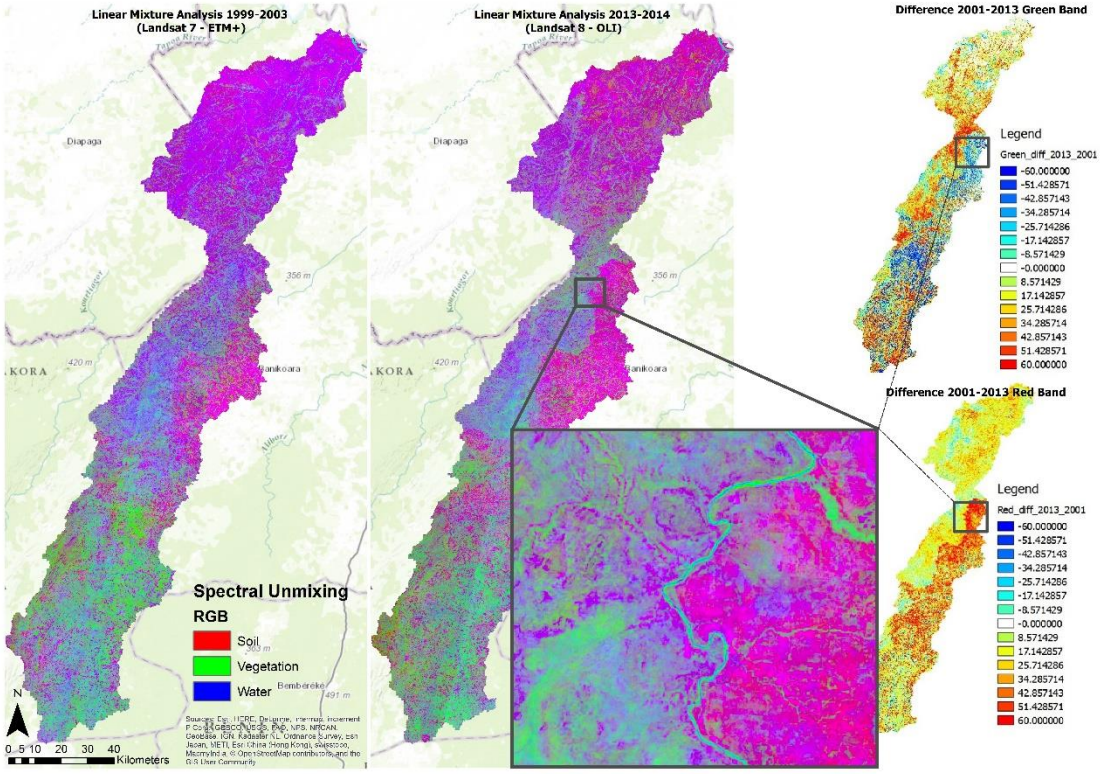

Figure 39. Spectral Unmixing (Soil, Vegetation, Water)

Linear Mixing Analysis is also an accurate approach for detection of forest loss. A large number of deforested areas are readily visible in the eastern portion of Figure 39. The clearings are dominated by high bare soil fractions (in red) which show similar patterns compared to those seen in the previous section. Also, many clearings display the prototypical reticular shape caused by humans.

Differences between soil and vegetation bands in the linear unmixing product reveal a decrease of vegetation cover in the north, close to the border of the W national park and the difference of both images also show that Land Cover changes are concentrated in those areas were the hot spots were detected.

4.2.8.4 **Greenness seasonality (NDVI)**

VGT4AFRICA, organized by the Flemish Institute for Technological Research NV (VITO) as part of the VEGETATION for Africa, the Joint Research Centre (JRC) and MEDIAS-France, provides various products for land applications and environmental monitoring and uses EUMETCast as primary data delivery mechanism.

These products range from the basic 10-daily vegetation index or NDVI at 1 km resolution to more advanced added value products such as, for example, Leaf Area Index (LAI), Normalized Difference Vegetation Index (NDWI), Burt Area (BA), Vegetation Productivity Index (VPI), etc.

All products cover the African continent and are delivered at regular, 10 day intervals. The 10-days synthesis is a core concept of the Spot/Vegetation products. There are 3 periods of 10-days a month, numbered 01, 11, 21. Period 01 covers the 1st to the 10th day of the month, period 11 covers the 11th to the 20th and period 21 covers the 21st to the last day of the month.

The data set used in the 'Greenness Seasonality' section is the Normalized Difference Vegetation Index, one of the most widely used index in Remote sensing vegetation monitoring that shows seasonal changes in vegetation and depicts health of vegetation and growing conditions.

The greening-up of vegetation starts in April and is markedly increased by August, when it starts declining until March (Figure 40), showing a clear dependence on precipitation patters shown in previous figures (26). Figure 41 shows these NDVI evolution for different land cover classes that were retrieved from ESA´s CCI viewer http://maps.elie.ucl.ac.be/CCI/viewer/index.php

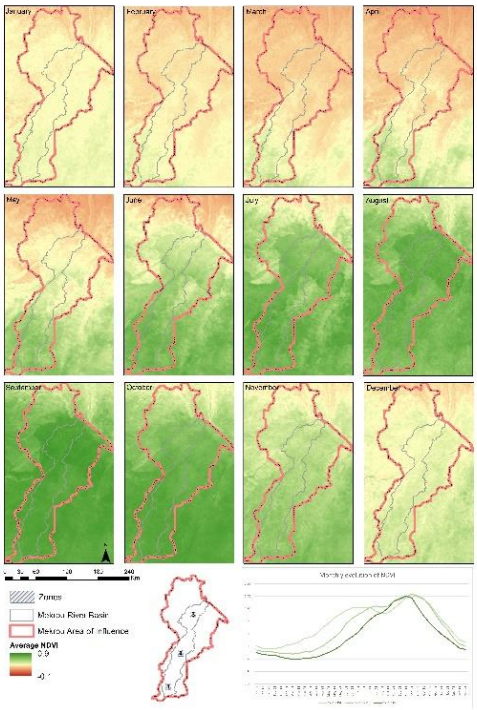

Figure 40. Greenness Seasonality (NDVI)

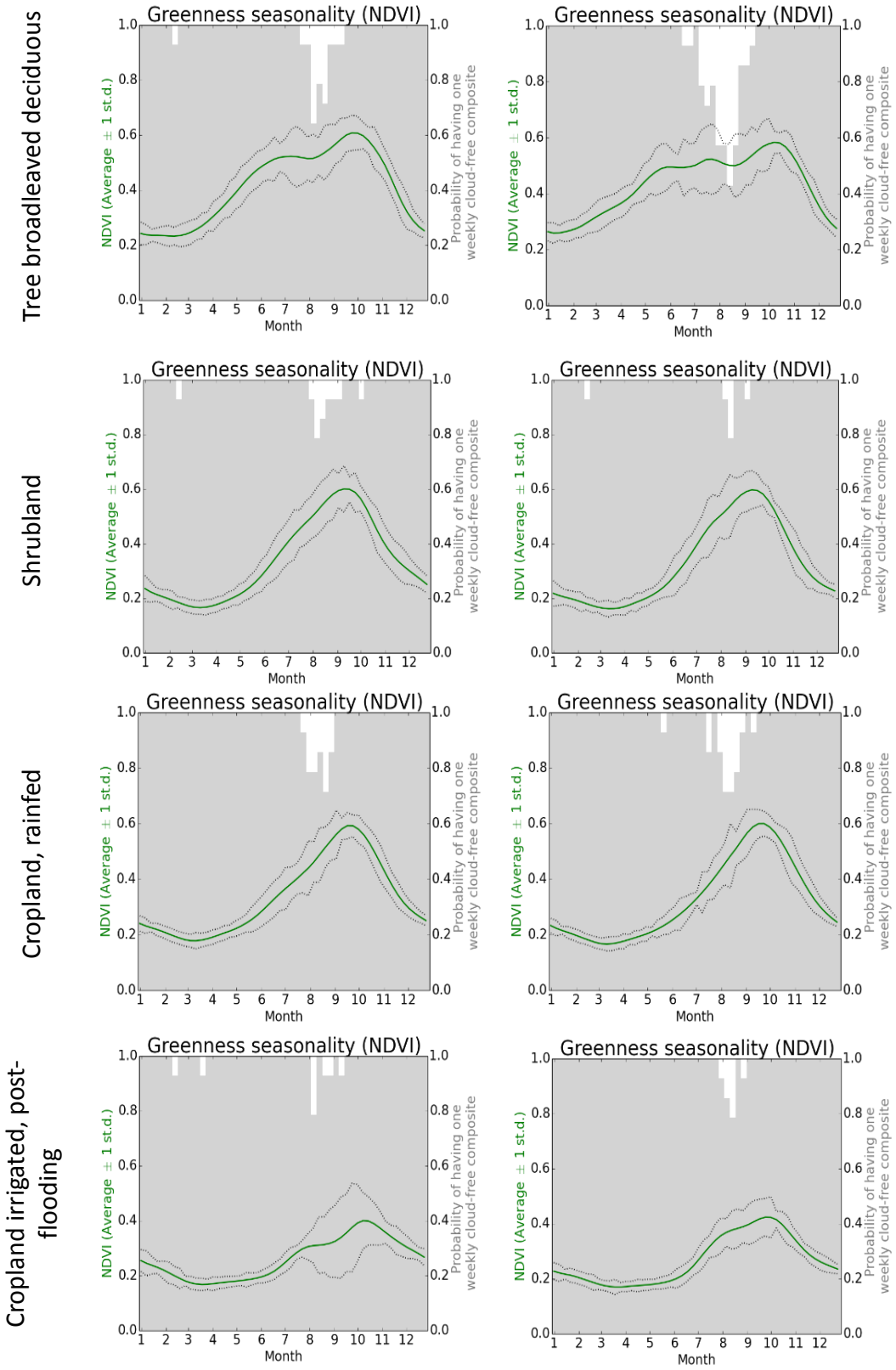

Figure 41. Greenness seasonality for different land cover classes

5 Additional added value maps

5.1 Priority of Irrigation

A first indicator for the identification of potential areas where irrigation equipment was derived by using available dataset and derived information is based on:

5.1.1 *Water availability index*

A multicriteria indicator of topographic and hydrological water availability calculated based on distance from nearest river stream (also differentiated with average discharge); elevation above nearest stream (as an indicator of need to pump water if needed);

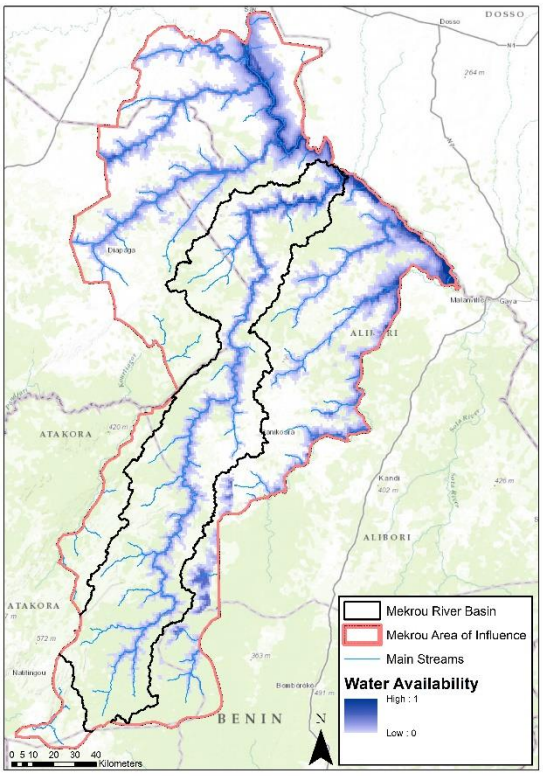

Figure 42. Water availibility Indicator

The map was calculated as follows:

i. Compute distance from nearest stream of a given magnitude (average yearly flow) D_Q (for simplicity we use 5 magnitude classes Q=0.1, 1, 10, 100, and 1000 m3/s)
ii. Compute elevation above nearest stream of that magnitude Z_Q
iii. Normalize distances and elevation differences

$D^*_Q = \min(1, D_Q/\text{thresh\_D})$

$Z^*_Q = \min(1, Z_Q/\text{thresh\_Z})$

Where thresh_D_Q and thresh_Z_Q are appropriate thresholds reflecting the max. distance, resp. elevation difference that can be accepted to withdraw water from a stream of magnitude Q.

iv. Compute a compound indicator of distance and elevation difference

$D^*=\sum_{Q=0.1}^{Q=1000}(\log Q + 2)\ (1 - D *_Q)$

$Z^*=\sum_{Q=0.1}^{Q=1000}(\log Q + 2)\ (1 - Z *_Q)$

v. Compute a weighted combination of Z* and D* reflecting the relative weight (cost) w of pumping (Z) over ditching/piping (D):

A = 1/ min (Z* , D*)

Compute the ratio S / A = S * min (Z* , D*)

Discharges Q are estimated by downscaling of LISFLOOD flow to streams per unit area

5.1.2 *Crop productivity under different irrigation scenarios*

EPIC model output (first year activity) were used to identify cell where potentially is convenient to increase irrigation as it would correspond to a high increase in the crop yield. High relative changes in crop productivity with free irrigation scenario means high potential and also high crop sensitivity to water);

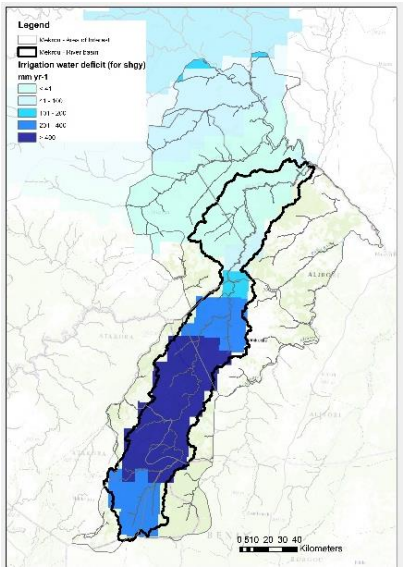

Figure 43. Volume of water required by crop for optima growth (mm/yr)

Irrigation water volume required under a potential optimal growing scenario for different crops. Here Map for Sorghum is reported (other layers and crops available in the Geodababase).

5.1.3 *Current distribution of irrigation equipment*

The map of area equipped for irrigation around the year 2005 in percentage of the total area (with a resolution of 5 minutes) was used a reference layers indicating where area already equipped are present (*Global Map of Irrigation Areas version 5).* Available Online: http://www.fao.org/nr/water/aquastat/irrigationmap/)

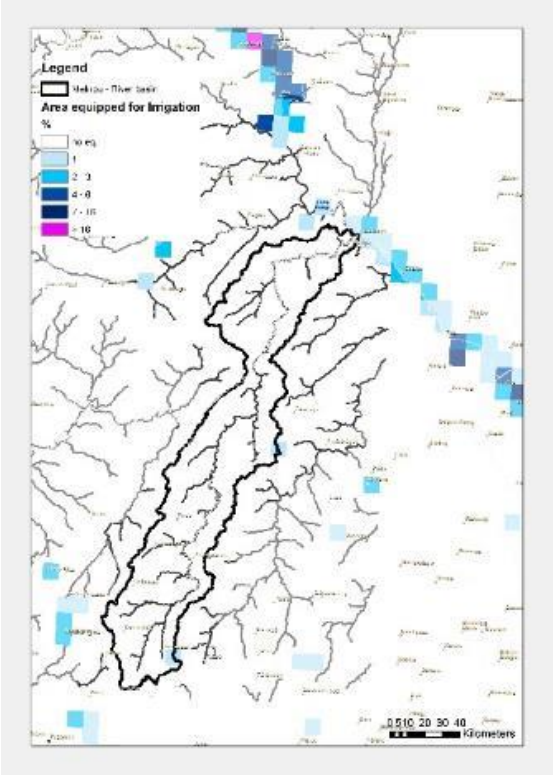

Figure 44. Area equipped for Irrigation

The map shows the amount of area equipped for irrigation around the year 2005 in percentage of the total area on a raster with a resolution of 5 minutes.

Additional available map layers refer to the percentage of the area equipped for irrigation that was actually used for irrigation and the percentages of the area equipped for irrigation that was irrigated with groundwater, surface water or non-conventional sources of water [30].

According to FAO data no area is currently equipped for irrigation except the northern area around the Niger River.

These three indicators were scaled in order to have a range 0-1 and multiplied to obtain a single unique indicator of areas were irrigation can be potentially expanded and where can bring to an efficient agricultural production increase.

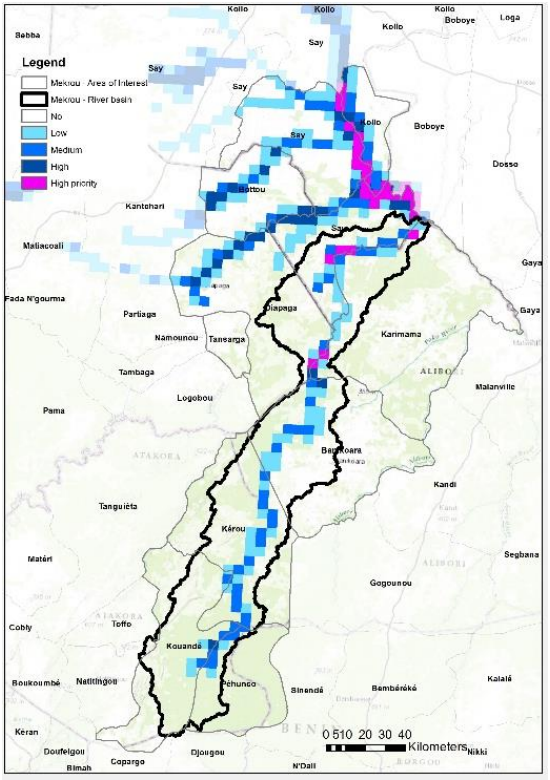

Figure 45. Priority areas for irrigation expansion

5.2 **Floodplains - A preliminary analysis of probability of flooding**

The objective of this preliminary analysis was to identify

- An indicator of probability of flooding due to high flows in the nearby channels is the rise in the channel water level that could exceed local elevation
- By using the 30m DEM with two analysis functions “buffering by elevation change” and “depression filling”

An indicator of probability of flooding due to high flows in the nearby channels is the rise in the channel water level that would exceed local elevation.

If a site is at lower elevation than a given channel water level and there is no higher obstacle between the channel and the site, the probability of that level to induce flooding is high.

A preliminary analysis was conducted on the basis of the DEM with two analysis functions known as “buffering by elevation change” and “depression filling”.

Both functions may be applied to individual pixels of a DEM. The calculation requires prior definition of a grid of pixels representing the stream network. This has been obtained by applying to the flow accumulation map derived from the DEM. Whether a

given pixel is at lower elevation than the one of the nearest pixel representing a stream channel, increased by a fixed quantity (for example 1 to 10 m increase) it identify a potential risk.

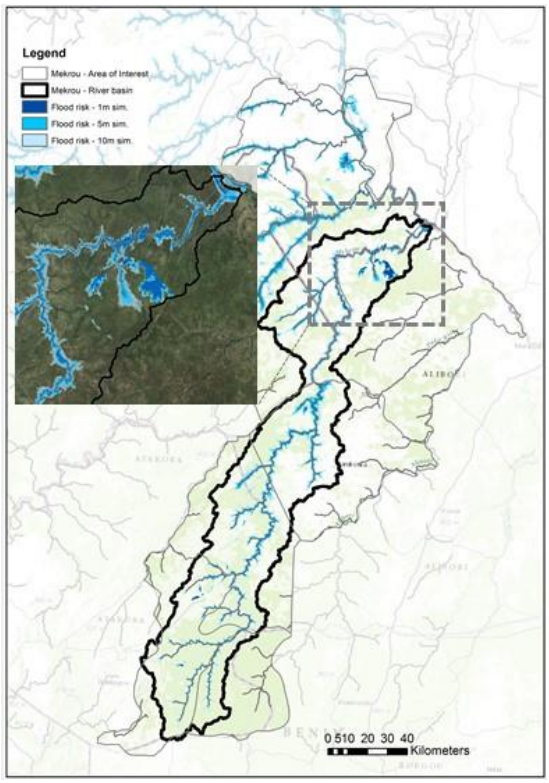

Figure 46. DEM indicator for flooding

5.3 **Agriculture**

5.3.1 ***Crop management***

Crop management is one of the most important sets of input required. It consists of detailed schedules and characteristics of the most common crop operations including sowing, harvesting, tillage, fertilisation, and irrigation, for each of the crop used in the region. Detailed data on crop calendars for the Mékrou region are missing (such data should be available after household survey). However, sub-national data were collected from public databases for most important crop. In the case of missing data for crop calendars a methodology was applied to derive most important crop calendar operational data (sowing, tillage, harvesting) based on:

- The total number of heat units required to bring a plant to maturity using long term minimum/maximum temperatures, optimum and minimum plant growing temperatures and the average number of days for the plant to reach maturity.

- A predefined minimum amount of rain occurred in 3 consecutive decades. In this case thresholds are differentiated according to annual rain.

5.3.1.1 Crop Calendars examples

Here is an example crop calendar (extracted from http://www.fao.org/agriculture/seed/cropcalendar/) for Benin agro-ecological zone of South Borgou for some cereals crop. Maps of different regions with specific crop calendars (locally defined) would be need.

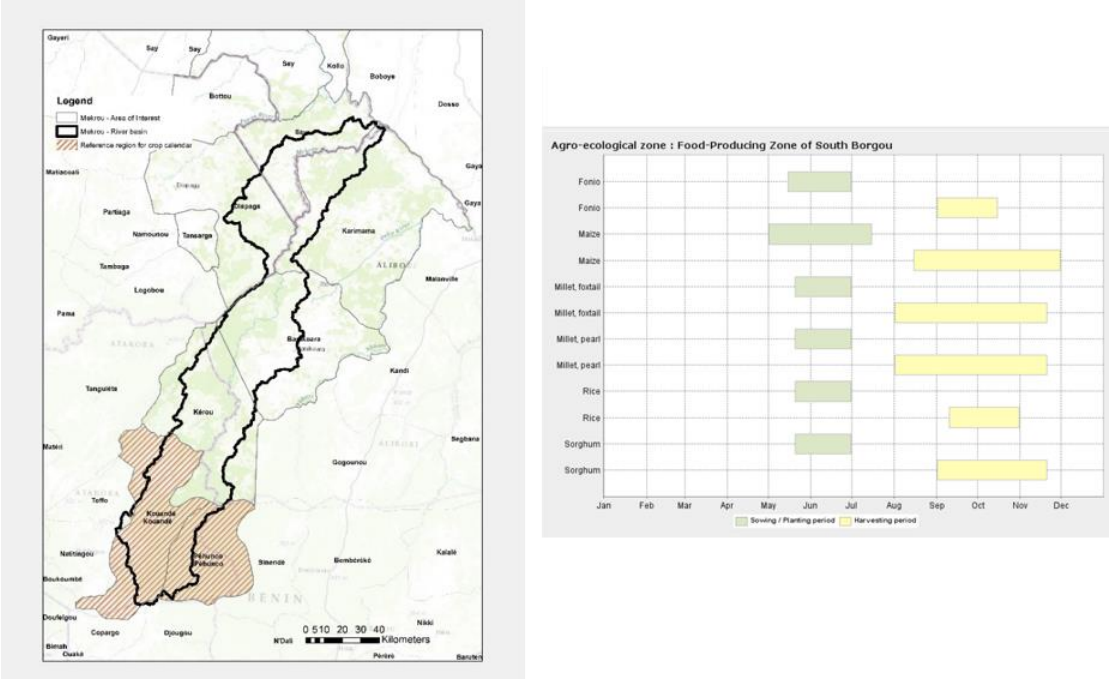

Figure 47. Ref region for crop calendar 1

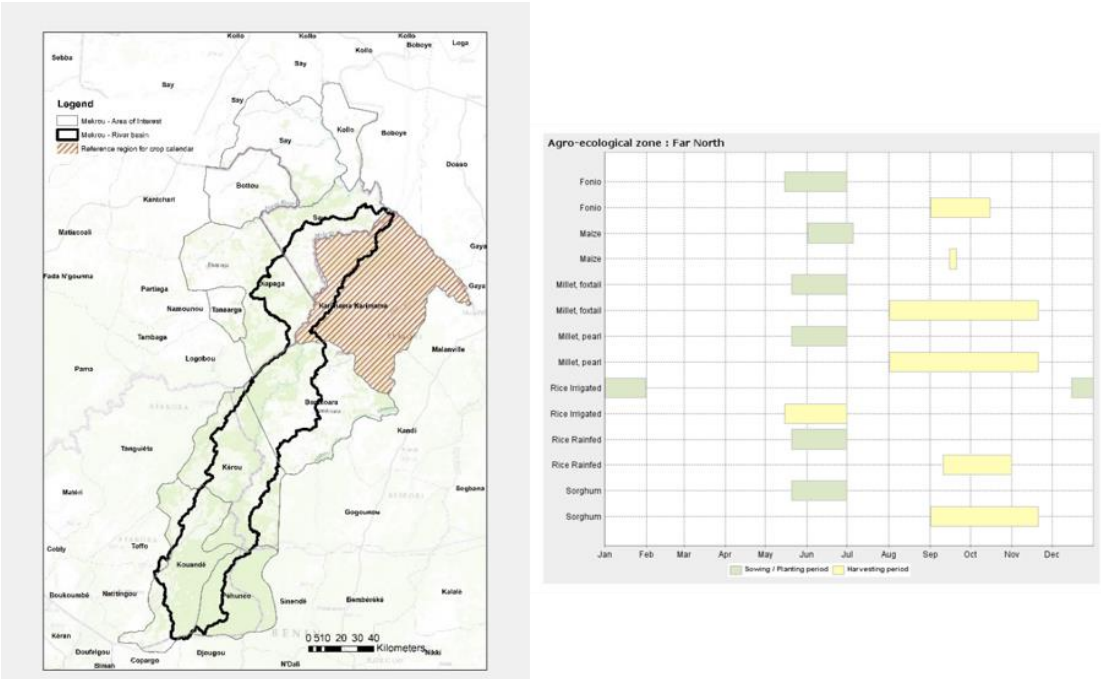

Figure 48. Ref. crop calendar 2 for cereals

5.3.2 *Crop / Pasture land*

The map shows the current cropland and pasture share in the region. Map is derived by data from a global dataset for year 2000 at a spatial resolution of about 10 km (5 min).

Agricultural inventory data and satellite-derived land cover data were used to train a land cover classification data set obtained by merging two different satellite-derived products (Boston University's MODIS-derived land cover product and the GLC2000 data set).

According to this data about 135000 ha of the river basin are classified as cropland, that means only about 13% of the river basin is currently used as cultivated land.

65100 ha area classified as pasture area corresponding about 6% of total river basin area.

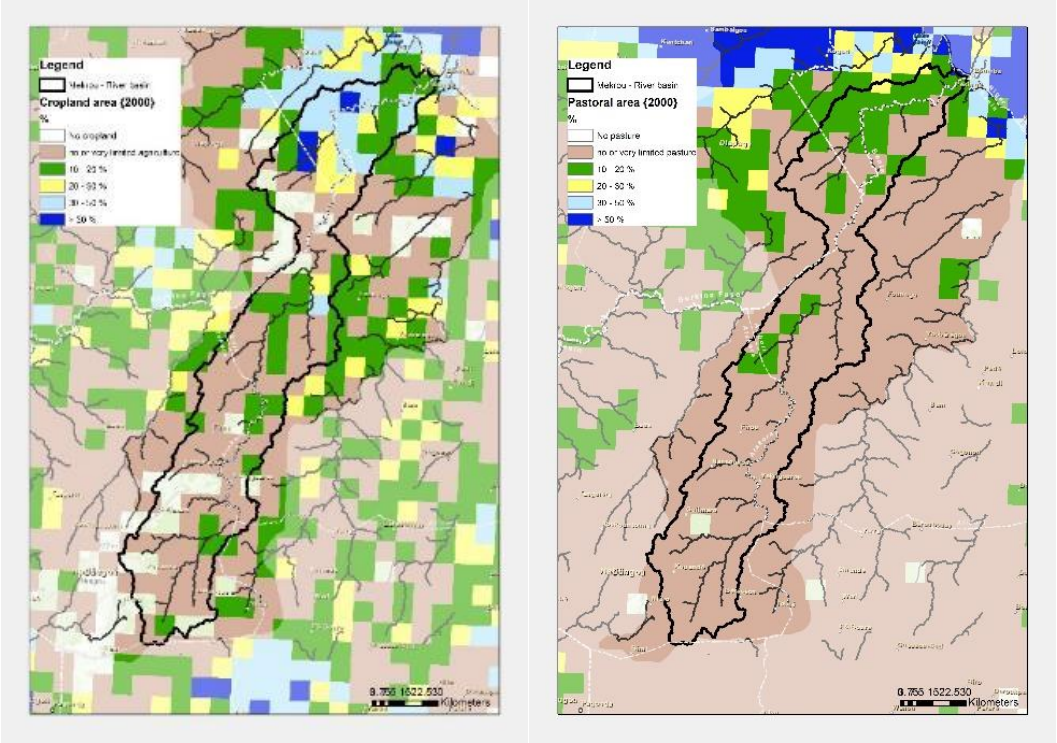

Figure 49. Pasture, Land share grid (5' res.)

5.4 **Livestock**

Livestock contributes directly to the livelihoods and food security of almost a billion people. In developing countries, the meat and dairy sectors have grown at average yearly rates of 5.1 percent and 3.6 percent respectively since 1970.

Detailed information on livestock density and distribution is essential for an effective management of water and food agriculture in the basin. At this stage we used the new global distribution maps at 1 km resolution for cattle, pigs and chickens available at http://www.livestock.geo-wiki.org/.

This dataset is derived from the more up-to date and detailed sub-national livestock statistics and it is based on a new and higher resolution set of predictor variables [31].

Here some example maps and statistics:

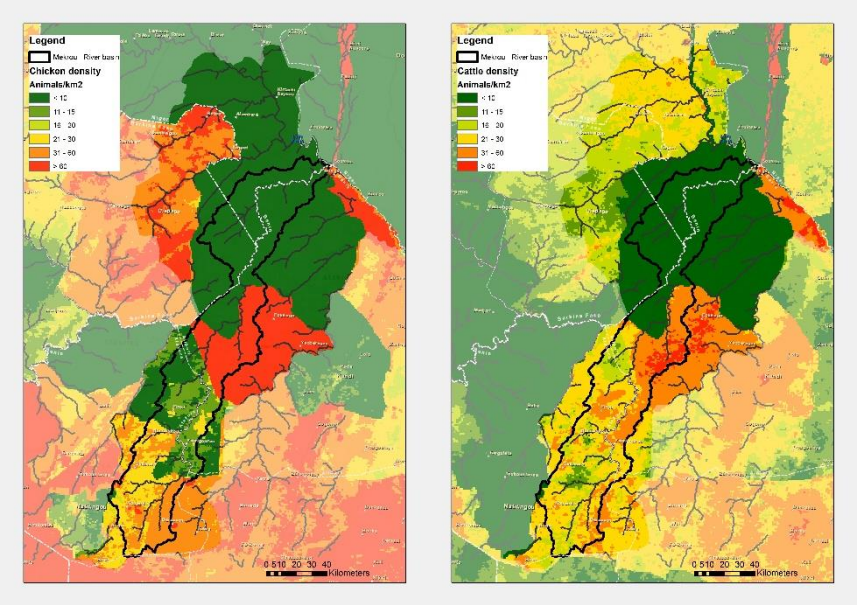

Figure 50. Chickens desnity Figure 51. Cattle density

Statistics by Administrative Communes

ISO	COUNTRY	NAME_1	NAME_2	NAME_3	OBJECTID_1	AVG Cattle density	Area km2	Tot Cattle	Avg Chicken density	Tot chickens
BEN	Benin	Atakora	Kérou	Kérou	1	25.2	3857.0	97197	13.5	52070
BEN	Benin	Atakora	Kouandé	Kouandé	2	22.2	3238.0	71883	28.8	93254
BEN	Benin	Atakora	Péhunco	Péhunco	3	28.2	2081.5	58699	42.6	88673
BEN	Benin	Alibori	Karimama	Karimam	4	7.2	5920.7	42629	16.1	95324
BEN	Benin	Alibori	Banikoara	Banikoar	5	41.3	4379.8	180886	107.2	469514
BFA	Burkina Faso	Tapoa	Bottou	Bottou	6	18.5	1873.3	34655	60.0	112395
BFA	Burkina Faso	Tapoa	Diapaga	Diapaga	7	6	3984.3	23906	21.2	84467
BFA	Burkina Faso	Tapoa	Tansarga	Tansarga	8	18.4	579.7	10667	79.6	46146
NER	Niger	Tillabéry	Kollo	Kirtachi	9	16.3	1026.3	16728	0.6	616
NER	Niger	Tillabéry	Say	Tamou	10	22.8	2792.5	63668	1.1	3072
NER	Niger	Tillabéry	Say	Parc W	11	0.7	2341.2	1639	0.1	234

Table 11. Livestock statistic data derived by modelled livestock density Maps.

5.5 Nitrogen availability from livestock

Agricultural production is mainly limited by water and nutrient availability. The available manure of livestock present in the river basin is a valid source of nitrogen that with an efficient management can potentially boost crop production. In order to quantify this level of fertilization in the river basin it was applied a simple estimation as described below.

The total number of animals available for each animal class was derived by 1 km resolution density distribution map [31]. For each animal class an average N production factor was used as follows:

Total N from livestock = n.of cattle * 50 kg N yr + n.of pigs * 12kg N yr + n.of Goats/sheep * 10 kg N yr + n.of chicken * 0.6 kg N yr.

Limited Distribution

The resulting map illustrates that potentially there is a moderate availability of N from livestock mainly in the following regions: Bottou, Banikoara, Kérou, Péuncho, Gaya.

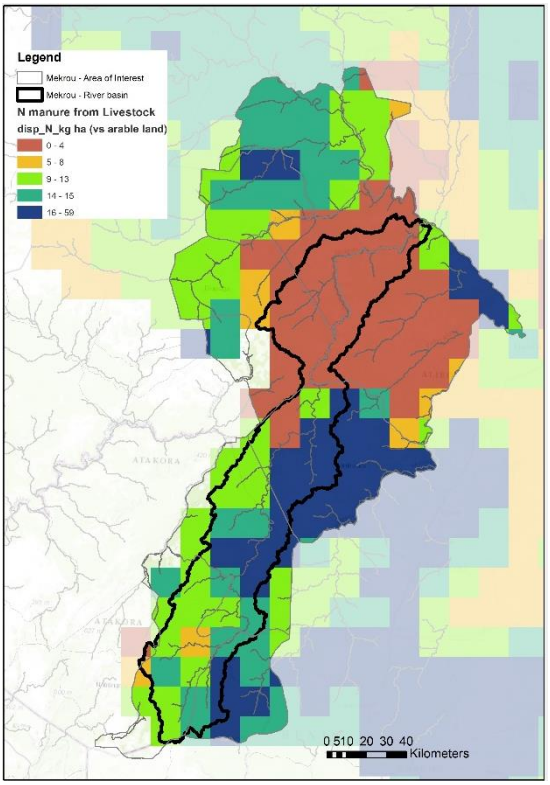

Figure 52. Nitrogen availability

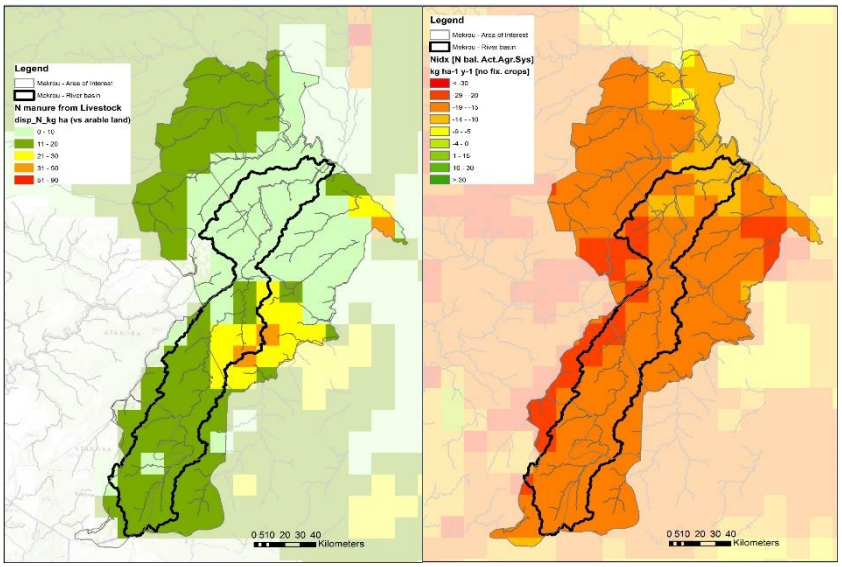

Figure 53. Nitrogen index and Nitrogen manure from Livestock

5.6 Erosion Risk

Soil erosion by water is an important and globally diffused problem. The assessment and quantification of this issue it's complex and filed measurements and surveys are expensive and difficult to transfer to regional and wider scales.

The Revised Universal Soil Loss Equation (RUSLE; Renard et al., 1997) is an empirically based model, founded on the Universal Soil Loss Equation (USLE; Wischmeier and Smith, 1978).

RUSLE computes the average annual erosion expected on hillslopes by multiplying several factors together: rainfall erosivity (R), soil erodibility (K), slope length and steepness (LS), cover management (C), and support practice (P).

The average soil loss due to water erosion per unit area per year (Mg ha−1 per year) was quantified, using RUSLE (USDA-ARS, 2001; Renard et al., 1997) by the following equation: A = R × K × L × S × C × P where:

R the rainfall and runoff erosivity factor (MJ mm ha−1 h−1 per year),

K the soil erodibility factor (Mg h MJ−1 mm−1),

L the slope length (m), S the slope steepness (%),

C the cover and management practice factor,

and P the support practice. RUSLE.

5.6.1 ***R – Rainfall Erosivity***

The R-factor, expressing erosive force of rainfall, is usually calculated as an average of EI values measured over 20 years to accommodate apparent cyclical rainfall patterns. Since Mékrou catchment region did not have long-term rainfall records, the R-factor was computed using the following procedure:

a) Reference literature R-values were collected over the African continent; only long term multi annual derived values were considered;
b) A linear regression was tested by considering reference data for stations: latitude, longitude, elevation, annual precipitation, and different statistics over the annual series (maximum monthly precipitation, 80th percentile, etc.)
c) The optimal regression was used to spatially calculate R factor over Mékrou region by considering data from locally detailed available input dataset (local precipitation data at 1km resolution, elevation from DEM at 30m resolution).

The resulting equation used to extrapolate R factor is:

$$R = \alpha + \beta * \ln\left(Rain_{month\_max}\right) + \gamma * Elev$$

Where α,β,γ are the coefficient of the regression optimized with the least squares method and are:

α= *-870.9*; β=*3588.401*; γ=*-1.65253*; $Rain_{month\_max}$= maximum monthly precipitation (over the observed period); [mm]; Elev= Station altitude in [m].

R^2 = 0.85; std = 1538

5.6.2 *K – Soil erodibility*

The K factor is an empirical measure of soil erodibility as affected by intrinsic soil properties. The main soil properties affecting K are soil texture, organic matter, structure, and permeability of the soil profile. Soil erodibility (K factor) was estimated based on the Kuery Software (see Borselli et al., 2012)

Soils in the region result in low values of erodibility (range is 0.006 to 0.025).

5.6.3 *LS – slope length/slope steepness*

The LS factor was calculate based on a simplified method, proposed by Moore and Wilson (1992) to derive a *LS* factor suitable for 3D application:

$$LS3 = \left(\frac{A_s}{22.13}\right)^m \left(\frac{\sin\theta}{0.0896}\right)^n$$

where the hillslope length is replaced by an accumulation area per contour length A_s (m^2/m); the exponent *m* may vary in the range 0.4-0.6 (0.4 for this analysis) ; and *n* varies in 1.2-1.3 (1.3 for this analysis).

5.6.4 *C – Cover Management factor*

The vegetation cover and management factor C represent the effect of cropping and management practices in agricultural management, and the effect of ground, tree, and grass covers on reducing soil loss in non-agricultural situation. For this analysis C factor was associated to each cell according to dominant land cover class.

Landuse	C
Rainfed cropland	0.3
Mosaic cropland	0.3
Vegetation (mosaic)	0.25
Open broadleaved forest	0.01
Forest/shrubland	0.01
grassland/forest	0.01
shrubland	0.05
grassland/forest	0.01

Table 12. Vegetation cover and management factor

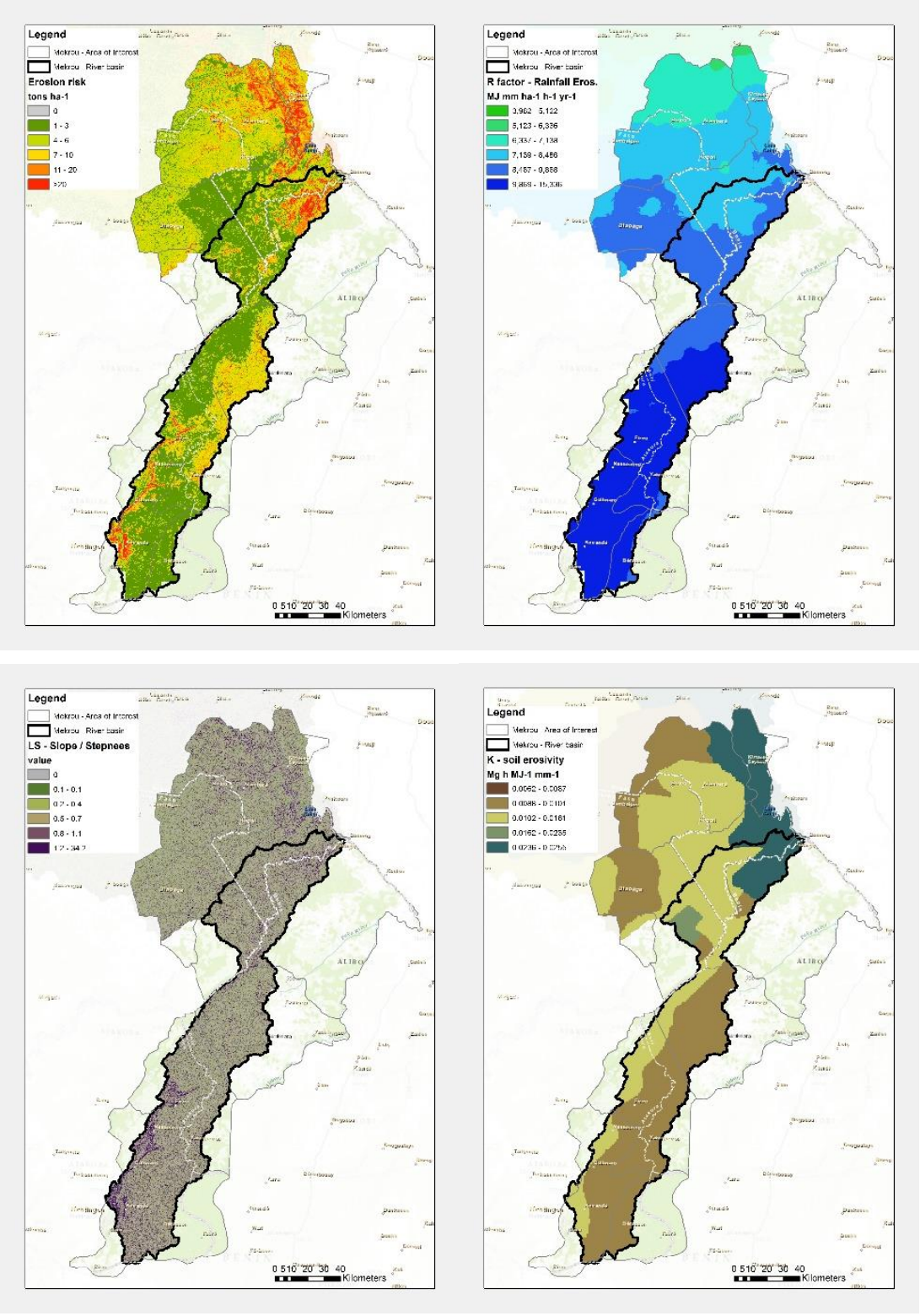

Figure 54. Erosion Risk Figure 55. Rain Erosivity Figure 56. LS – slope length/slope steepness Figure 57. K – Soil erodibility

6 References

[1] GADM database of Global Administrative Areas, GADM v.2.5. Robert Hijmans in collaboration with Julian Kapoor and John Wieczorek (University of California, Berkeley), Nel Garcia, Aileen Maunaham, Arnel Rala (International Rice Research Institute) and Alex Mandel (University of California, Davis).

[2] IUCN and UNEP-WCMC (2013), *The World Database on Protected Areas (WDPA)* [On-line], [downloaded 06/2015, version 08/2013], Cambridge, UK: UNEP-WCMC. Available at: www.protectedplanet.net

[3] J-M. Grégoire et D. Simonetti (2007). Dynamique des brûlis dans le Parc Régional du W, le Parc national de La Boucle de la Pendjari et la Réserve d´Arly, Implications pour la gestión de ces aires protégées. JRC 40526. Joint Research Centre, European Commission.

[4] Reynaud et al (2015) Combining expert and stakeholder knowledge to define wáter management priorities in the Mékrou River Basin. MDPI-AG, ISSN 2073-4441. DOI: 10.3390/w7126675.URI
http://publications.jrc.ec.europa.eu/repository/handle/JRC97855

[5] This product was made utilizing the LandScan 2013™ High Resolution global Population Data Set copyrighted by UT-Battelle, LLC, operator of Oak Ridge National Laboratory under Contract No. DE-AC05-00OR22725 with the United States Department of Energy. The United States Government has certain rights in this Data Set. http://www.ornl.gov/landscan/

[6] Nelson, A. (2008) Estimated travel time to the nearest city of 50,000 or more people in year 2000. Global Environment Monitoring Unit - Joint Research Centre of the European Commission, Ispra Italy. Available at http://forobs.jrc.ec.europa.eu/products/gam/ (accessed 06/2015).

[7] Sayre and others. 2014. A New Map of Global Ecological Land Units — An Ecophysiographic Stratification Approach. Washington, DC: Association of American Geographers. 46 pages.

[8] NASA Land Processes Distributed Active Archive Center (LP DAAC) Products. *These data are distributed by the Land Processes Distributed Active Archive Center (LP DAAC), located at USGS/EROS, Sioux Falls, SD. http://lpdaac.usgs.gov*

[9] Lehner, B., Verdin, K., Jarvis, A. (2008): New global hydrography derived from spaceborne elevation data. Eos, Transactions, AGU, 89(10): 93-94. http://hydrosheds.cr.usgs.gov/index.php

[10] Lehner, B., Verdin, K., Jarvis, A. (2008): New global hydrography derived from spaceborne elevation data. Eos, Transactions, AGU, 89(10): 93-94.

[11] Lehner, B., Grill G. (2013): Global river hydrography and network routing: baseline data and new approaches to study the world's large river systems. Hydrological Processes, 27(15): 2171–2186.

[12] EUROCLIMA Project. Available online: http://www.euroclima.org/en/euroclima (accessed on 12 December 2014).

[13] CHIRP. Available online: http://chg.geog.ucsb.edu/data/chirps/ (accessed on 20 August 2014).

[14] Ceccherini, G.; Ameztoy, I.; Hernández, C.P.R.; Moreno, C.C. High-Resolution Precipitation Datasets in South America and West Africa based on Satellite-Derived Rainfall, Enhanced Vegetation Index and Digital Elevation Model. *Remote Sens*. **2015**, *7*, 6454-6488

[15] WorldClim version 1 was developed by Robert J. Hijmans, Susan Cameron, and Juan Parra, at the Museum of Vertebrate Zoology, University of California, Berkeley, in collaboration with Peter Jones and Andrew Jarvis (CIAT), and with Karen Richardson (Rainforest CRC).

[16] Global Runoff Data Centre ([*2015*]): [*Long-Term Mean Monthly Discharges and Annual Characteristics of GRDC Stations*] / *Global Runoff Data Centre. Koblenz, Federal Institute of Hydrology (BfG),* [2015]. Dataset acquired under a cooperation agreement between the GRDC and the Climate Risk Management and Water Units, IES-JRC.

[17] Improvements to a MODIS Global Terrestrial Evapotranspiration Algorithm Mu, Q., M. Zhao, S. W. Running Remote Sensing of Environment, Volume 115, pages 1781-1800 (doi:10.1016/j.rse.2011.02.019) http://www.ntsg.umt.edu/project/mod16

[18] Zomer RJ, Trabucco A, Bossio DA, van Straaten O, Verchot LV, 2008. Climate Change Mitigation: A Spatial Analysis of Global Land Suitability for Clean Development Mechanism Afforestation and Reforestation. Agric. Ecosystems and Envir. 126: 67-80. CGIAR-CSI website (http://www.cgiar-csi.org)

[19] UNEP (United Nations Environment Programme), 1997. World atlas of desertification 2ED. UNEP, London.

[20] Mahé G., Bamba F., Orange D., Fofana L., Kuper L., Marieu B., Soumaguel A. & Cissé 2002. Dynamique hydrologique du Delta Intérieur du Niger Mali. *In* D. Orange, R. Arfi, M. Kuper, P. Morand & Y. Poncet. eds. *Colloques et séminaires*, Éditions de l'IRD, Paris. (à paraître).

[21] Hartmann, Jörg; Moosdorf, Nils (2012): Global Lithological Map Database v1.0 (gridded to 0.5° spatial resolution). doi:10.1594/PANGAEA.788537, Supplement to: Hartmann, Jens; Moosdorf, Nils (2012): The new global lithological map database GLiM: A representation of rock properties at the Earth surface. Geochemistry, Geophysics, Geosystems, 13, Q12004, doi:10.1029/2012GC004370

[22] Fan, Y., Li, H. & Miguez-Macho, G., 2013. Global patterns of groundwater table depth. Science, 339(6122), pp.940–943. Available at: http://www.ncbi.nlm.nih.gov/pubmed/23430651.

[23] Fischer, G., F. Nachtergaele, S. Prieler, H.T. van Velthuizen, L. Verelst, D. Wiberg, 2008. Global Agro-ecological Zones Assessment for Agriculture (GAEZ 2008). IIASA, Laxenburg, Austria and FAO, Rome, Italy.

[24] Di Gregorio, A.; Jansen, L.J. Land Cover Classification System (LCCS): Classification Concepts and User Manual; Food and Agriculture Organization of the United Nations: Rome, Italy, 2000.

[25] Congalton, R.G.; Gu, J.; Yadav, K.; Thenkabail, P.; Ozdogan, M. Global Land Cover Mapping: A Review and Uncertainty Analysis. *Remote Sens.* **2014**, *6*, 12070-12093.

[26] ISRIC – World Soil Information, 2013. SoilGrids: an automated system for global soil mapping. Available for download at http://soilgrids1km.isric.org.

[27] Hengl T, de Jesus JM, MacMillan RA, Batjes NH, Heuvelink GBM, et al. (2014) SoilGrids1km — Global Soil Information Based on Automated Mapping. PLoS ONE 9(8): e105992. doi:10.1371/journal.pone.0105992

[28] Jun Chen, et.al. Global land cover mapping at 30 m resolution: A POK-based operational approach. ISPRS Journal of Photogrammetry and Remote Sensing. Volume 103, May 2015, Pages 7–27 doi:10.1016/j.isprsjprs.2014.09.002 - GlobeLand30 (GLC30) National Geomatics Center of China 2014. http://www.globallandcover.com/

[29] Hansen, M. C., P. V. Potapov, R. Moore, M. Hancher, S. A. Turubanova, A. Tyukavina, D. Thau, S. V. Stehman, S. J. Goetz, T. R. Loveland, A. Kommareddy, A. Egorov, L. Chini, C. O. Justice, and J. R. G. Townshend. 2013. "High-Resolution Global Maps of 21st-Century Forest Cover Change." Science 342 (15 November): 850–53. Data available on-line from: http://earthenginepartners.appspot.com/science-2013-global-forest.

[30] Stefan Siebert, Verena Henrich, Karen Frenken and Jacob Burke (2013). *Global Map of Irrigation Areas version 5.* Rheinische Friedrich-Wilhelms-University, Bonn, Germany / Food and Agriculture Organization of the United Nations, Rome, Italy.Available Online: http://www.fao.org/nr/water/aquastat/irrigationmap/

[31] Robinson TP, Wint GRW, Conchedda G, Van Boeckel TP, Ercoli V, Palamara E, et al. (2014) Mapping the Global Distribution of Livestock. PLoS ONE 9(5): e96084. doi:10.1371/journal.pone.009608

R.Laë et. al. Review of the Present State of the Environment, Fish Stocks and Fisheries of the River Niger (West Africa). Proceedings of the second inter-annual symposium on the management of large rivers for fisheries. 11th-14th February 2003. FAO Corporate document repository.

Edoardo Simonetti, Dario Simonetti, Damiano Preatoni, 2014. Phenology-based land cover classification using Landsat 8 time series. JRC Technical Reports

European Commission

Joint Research Centre

Institute for Environment and Sustainability

Contact information

César Carmona-Moreno

Address: Joint Research Centre, Via Enrico Fermi 2749, TP 440, 21027 Ispra (VA), Italy

E-mail: cesar.carmona-moreno@jrc.ec.europa.eu

Tel.: +39 0332 78 9654

Fax: +39 0332 78 9073

http://ies.jrc.ec.europa.eu/

http://www.jrc.ec.europa.eu/

This publication is a Reference Report by the Joint Research Centre of the European Commission.

As the Commission's in-house science service, the Joint Research Centre's mission is to provide EU policies with independent, evidence-based scientific and technical support throughout the whole policy cycle.

Working in close cooperation with policy Directorates-General, the JRC addresses key societal challenges while stimulating innovation through developing new standards, methods and tools, and sharing and transferring its know-how to the Member States and international community.

Key policy areas include: environment and climate change; energy and transport; agriculture and food security; health and consumer protection; information society and digital agenda; safety and security including nuclear; all supported through a cross-cutting and multi-disciplinary approach.